THE PENNSYLVANIA STATE UNIVERSITY
SCHREYER HONORS COLLEGE

Influence of Crosslinker Concentration on Properties of Shape Memory Poly(cyclooctene) (PCO).

KAROLINE ROETTGER
FALL 2025

A thesis
submitted in partial fulfillment
of the requirements
for a baccalaureate degree
in Chemical Engineering
with honors in Chemical Engineering

Reviewed and approved* by the following:

Patrick T. Mather, Ph.D.
Professor of Chemical Engineering
Thesis Supervisor

Dr. Ali Borhan
Professor of Chemical Engineering
Thesis Honors Adviser

* Electronic approvals are on file.

Abstract

This thesis investigates the influence of crosslinker concentration, dicumyl peroxide (DCP), on the thermal, mechanical, and shape memory properties of polycyclooctene (PCO), a semicrystalline elastomer with potential biomedical applications. By varying the amount of dicumyl peroxide (DCP) used during processing, polymer networks with different crosslink densities were synthesized and characterized. Thermal properties were examined through differential scanning calorimetry (DSC), while dynamic mechanical analysis (DMA) was used to quantify storage modulus, loss modulus, and shape memory performance. Gel fraction measurements confirmed successful network formation and helped form the most efficient network by removing loose chains.

The results show that increasing crosslink density decreases the degree of crystallinity, lowering the observed melting temperature while simultaneously enhancing mechanical recovery. DMA data demonstrated that higher DCP content led to improved shape recovery, with the most crosslinked samples exhibiting greater actuation strength and more complete recovery cycles. However, increased crosslinking also broadened hysteresis and slowed crystallization kinetics, suggesting a trade-off between recovery efficiency and responsiveness. Isothermal crystallization experiments further revealed that elongation is highly sensitive to small changes in temperature, showing the complex relationship between crosslink density, applied stress, and thermal conditions.

One promising area of application is the development of adaptive biomedical casting materials, particularly for pediatric clubfoot treatment, where tunable stiffness and controlled shape recovery are advantageous. Beyond biomedical devices, this work contributes to the

broader field of shape memory polymers by demonstrating how crosslinking chemistry can be used to trigger both thermal transitions and mechanical response.

TABLE OF CONTENTS

LIST OF FIGURES

LIST OF TABLES

ACKNOWLEDGEMENTS

I would like to start by expressing how deeply grateful I am to Penn State for giving me four unforgettable years filled with opportunities, lifelong friendships, and a place I've come to call home. This thesis represents the culmination of not just my academic work, but my personal growth as well. For three of four years of my undergraduate journey, I've had the privilege of being a part of the Mather Research Group, where I was given space to explore, question, and create. I joined the lab as a sophomore, excited for the chance to do hands-on research. What I found was even more meaningful, a place where my love of science and creativity could merge, and where I could truly contribute.

None of this would have been possible without the guidance of Dr. Patrick Mather. Dr. Mather has had one of the most meaningful influences on my undergraduate career. From the moment I joined the group, he encouraged me to be curious and bold in my research. He never made me feel like "just an undergraduate" but instead treated me like a real contributor to the work being done in the lab. Every meeting with Dr. Mather left me feeling energized with new ideas and confidence in my ability to pursue them. His feedback was thoughtful and constructive, and he always took the time to explain the bigger picture of the research, helping me understand not only what we were doing but why it mattered. Beyond the lab, Dr. Mather has been a mentor in the truest sense of the word. He offered guidance on my undergraduate career, career paths, and even life outside of engineering. I always looked forward to our conversations because I knew I would leave feeling more confident and supported. His enthusiasm for materials science is contagious, and he has a way of making even the most complex topics feel approachable and exciting. I'm incredibly lucky to have had a mentor who believed in me and gave me the

freedom to take ownership of my work. The lessons I learned from Dr. Mather—both technical and personal—will stay with me long after this thesis.

This thesis also would not exist without Dr. Sebanti Chattopadhyay. Her enthusiasm for research, constant encouragement, and willingness to meet with me (often daily) made this experience not only productive, but genuinely fun. Her positive attitude and openness to new ideas really made us a powerful team, we have come up with new ideas and procedures that I am very proud of. She answered every question I've thrown her way, helped me troubleshoot in the lab, and provided thoughtful feedback on more drafts of this thesis than I can count. I've learned so much from her, and I'm incredibly grateful for her mentorship, patience, and generosity.

Being a Schreyer Scholar has opened doors I never imagined. Schreyer gave me the platform to pursue independent research, which eventually led to multiple internships, connections with incredible mentors, and the confidence to pursue challenging goals. The support provided by Schreyer—from scholarships to advisors—has been invaluable. I've met some of the most driven and inspiring people through Schreyer events, and being a part of that community has pushed me to be better. Writing this thesis was one of the most difficult things I've done, but knowing I was part of a program that values depth, curiosity, and innovation kept me motivated. I'm proud to be a Schreyer Scholar and grateful for how it has shaped my undergraduate experience.

Research led me to my first internship at Dow Chemical, where I met Sarah Spengler, who quickly became like a big sister to me. The entire team at HRB made work exciting and interesting, supported my growth, and truly treated me like family. I'm also thankful for my time at Lockheed Martin, where the Process Control group welcomed me with open arms. Special thanks to Steve Almas, Gary Withaeger, Sheldon Watson, and Alexis Maldonado for giving me

hands-on experience I was able to use directly in this thesis, and for making every day in the lab exciting.

To everyone in the Mather Research Group: thank you for listening to countless research updates, literature reviews, and for offering support throughout this journey. Being part of such a collaborative and intellectually curious group made this work even more rewarding. And to the Penn State Chemical Engineering faculty and staff, thank you for pushing me, teaching me, and preparing me for what comes next.

To my roommates— Jordyn Sanders, Jen Miller, Elizabeth Long, and Varsha Rajan— you've been my family through every phase of college. I could not imagine better people to have by my side for all these years. We have gone through countless experiences together, and I truly consider them family. I can't wait to see what the future has in store for us, and I know we will face it all together! I am so honored to have friends that are caring, intelligent, fun, and truly there for me whenever I need them. Lodge forever, and the "Real Housewives of West College Ave" have left their mark on Penn State.

To my family: I don't have the words to say thank you enough. The Luca family—thank you for convincing me to come to Penn State. To my brother Roger and his wife Rachael, thank you for being my role model in chemical engineering, and for always guiding me with advice that led me to the right places, the right people, and the right opportunities—even if you both went to Ohio State. To my parents, thank you for absolutely everything. You've moved me across the country more times than I can count, come to visit me whenever I needed you, and pick up every phone call, whether I was celebrating or stressed-out walking across campus. You are my biggest supporters and the best parents I could ask for. From studying for the elapsed time test in third grade, so sitting with me through college applications, and to know supporting

me through the thesis process, none of this truly could be done without you. I am beyond lucky to have two intelligent and loving parents who have raised me in my Catholic faith along with instilling a confidence in me that will carry me through the next phases of my life. Like I said before, words cannot express how grateful I am for everything that they have done for me.

Penn State has truly been home. It's where I've grown into myself, where I've found my people, and where I've built a foundation that I'm proud of. I can't express how much this place and these people mean to me. Thank you for being part of the journey.

We Are!

Chapter 1

Introduction and Overview of Relevant Topics

1.1 Introduction to semi-crystalline crosslinked polymeric networks:

Polymers are macromolecules composed of repeating monomer units that form long chains or interconnected networks. Their molecular structure—ranging from linear arrangements to highly crosslinked structures—enables a wide variety of mechanical, thermal, and chemical properties, making them important in industries from packaging to aerospace. Crosslinking, which involves chemically bonding polymer chains, transforms these materials into robust networks with enhanced mechanical strength, thermal stability, and shape retention compared to their un-crosslinked counterparts (1). Crosslinking can be through chemical (such as covalent bonding) or physical (such as entanglements or crystallites) sources, both of which restrict chain mobility and influence polymer behavior.

Polymer networks are typically classified as either amorphous or semicrystalline based on their molecular organization (2). Amorphous polymers lack a well-defined structure, resulting in greater flexibility but lower stiffness; common examples include polystyrene (PS) and polycarbonate (PC). In contrast, semicrystalline polymers have both ordered crystalline regions and disordered amorphous regions, giving them a combination of mechanical strength and flexibility (3). Examples of semicrystalline polymers include polyethylene (PE) and polypropylene (PP). This balance is critical for many performance-based applications such as flexible tubing, high-strength fibers, and impact-resistant packaging.

During crystallization, polymer chains fold into lamellar structures that aggregate into ordered crystalline domains (see Figure 1.1). Crystallinity depends on factors like polymer

chemistry, molecular weight, processing methods, and cooling rate (4). The degree of crystalline regions influences the overall mechanical and thermal behavior of the semi-crystalline polymer network.

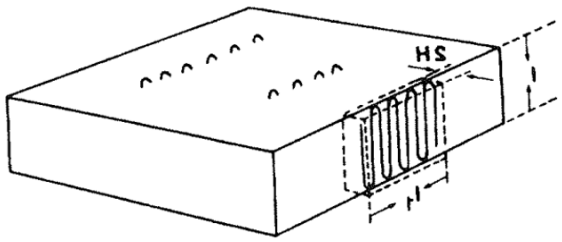

Figure 1: Figure illustrates the lamellar structure of polymer crystallites of polymer crystallite, depicting chain orientation in the direction normal to the crystal lamella along with "hairpin" folds of each crystallized chain. (18)

1.2 Elastomers and Shape Memory Polymers (SMPs)

Elastomers are a type of polymer network characterized by their ability to undergo large, reversible deformations. Structurally, they consist of loosely crosslinked polymer networks that provide both flexibility and resilience. These crosslinks act as anchors that allow the molecular chains to stretch under stress and recoil when the stress is removed, giving elastomers their signature elastic behavior (5). This combination of softness and recoverability makes them ideal for applications requiring durability and flexibility, such as seals, medical devices, and soft actuators. A comprehensive overview of elastomeric materials, including their design, synthesis, and mechanical properties, is provided by Zhao et al (12).

A specialized subset of elastomers is shape memory polymers (SMPs), which can "remember" and return to a permanent shape after being deformed and stored in a temporary shape. Their recovery is triggered by external stimuli such as temperature, light, moisture, etc.

(6). Not all elastomers exhibit the shape memory effect (SME). For SME to occur, the polymeric network must have both a switching phase—characterized by a thermal transition such as the glass transition temperature (Tg) or melting temperature (Tm)—and a stable network phase, such as chemical crosslinks or crystalline domains (4).

In semicrystalline SMPs, crystalline regions act as physical crosslinks that anchor the temporary shape, during cooling, in a process called “fixing”. Fixing the temporary shape is a key component of SME. Upon reheating, the polymer recovers its original shape as the polymeric chains regain mobility. During programming, the material is heated above the switching temperature and deformed, then cooled while holding the deformation constant. Once the cooling process completes, the chains get “fixed” into the deformed state storing the energy supplied to the network during the deformation. Upon reheating, the network uses this stored elastic energy to drive the transition back to its permanent shape (7).

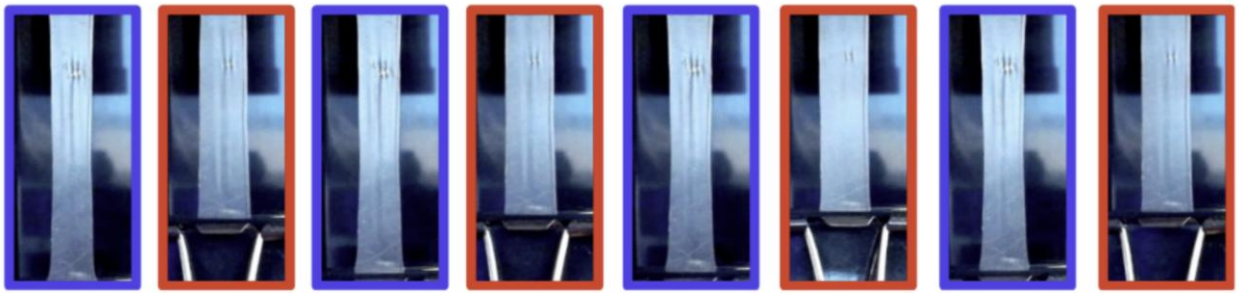

Figure 2: Demonstration of shape memory actuation in a crosslinked poly(cyclooctene) (PCO) strip. A clamped weight applies tension while thermal cycling drives reversible two-way SME: contraction in the heated state (red frames, left) and elongation in the cooled state (blue frames, right).

strip. A weight is clamped at the bottom (visible in the red-bordered frames) to apply tension. The red and blue borders represent heated and cooled states, respectively. The figure highlights

the reversible two-way shape memory behavior, where the polymer alternates between contraction and elongation during repeated thermal cycling (6).

Conventional shape memory polymers show a one-way SME where they lose any memory of their temporary shape once the material recovers its permanent shape upon reheating. However, SMPs can also be two-way or multi-way, wherein they can retain and switch between more than one shape. For instance, two-way SMPs can reversibly switch between two shapes under repeated heating and cooling cycles, as shown in Figure 1.2. Usually, an externally applied stress is required to guide and reinforce the directional shape change in two-way SMPs (8). However, there are polymeric systems that also exhibit stress-free two-way shape memory behavior.

1.3 Semicrystalline SMPs and the Role of Crosslinking

Semicrystalline SMPs with their hybrid morphology—containing both crystalline and amorphous regions—offer a tunable balance of stiffness and flexibility, making them highly desirable for practical applications. Crystalline regions serve as physical anchors that fix the temporary shape, while amorphous regions enable shape recovery upon heating (11). Increasing crystallinity generally enhances fixity and thermal stability but may reduce extensibility, making careful tuning essential.

Figure 3: Semicrystalline SMP showing both crystalline and amorphous regions (12).

1.4 Characterizing the shape memory effect in SMPs

Shape fixing and recovery are important components of shape memory polymers. Thus, to characterize SMPs based on these components, the following parameters are typically used: shape fixity ratio (Rf), shape recovery ratio (Rr), and switching temperature (Ts). Rf measures how well a temporary shape is held after removal of the deforming forces, while Rr indicates how well the original shape is recovered (see Figure 1.3). Ts is the temperature at which the material transitions from its fixed state back to its permanent shape. These metrics depend on factors such as polymer structure, crosslink density, crystallinity, and molecular weight (11). Thus, these parameters can be optimized suitably for tailoring SMPs to application-specific needs. For instance, biomedical devices may require a Ts near body temperature, along with high Rf and Rr values to ensure reliable shape change and recovery.

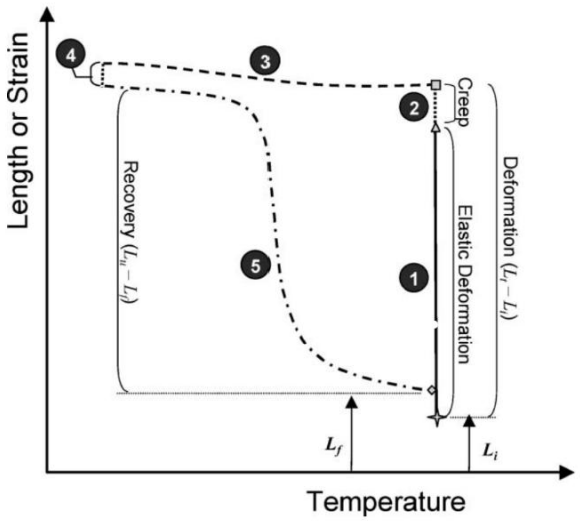

Figure 4: Figure shows the key shape memory metrics (as explained in the text) such as shape fixity and shape recovery ratios (Rf and Rr). (14)

1.5 Thermally Responsive SMPs

As mentioned previously, the shape memory effect in polymers can be triggered by various stimuli. For this thesis, we study thermo-responsive SMPs that switch shapes in response to external temperature. The switching temperature in this case can be either Tg or Tm. Tg marks the transition from a glassy, rigid state to a rubbery, flexible one, while Tm indicates the transition from a semi-crystalline to a rubbery, flexible one (10). SMPs based on melting temperature (Tm) rather than glass transition temperature (Tg) are ideal for applications requiring activation near physiological temperatures, such as biomedical devices like stents, sutures, or drug delivery systems. For example, polycyclooctene (PCO) is used because its Tm is close to body temperature, allowing for effective shape memory activation in biomedical environments.

1.6 Processing and Material Selection

Another important consideration in the mechanical behavior of elastomers is processing methods which can significantly influence crystallinity, orientation, and network formation. Common polymer processing techniques include melt extrusion, solution casting, and electrospinning (9). This thesis uses melt extrusion for its consistency and control over temperature, followed by thermal curing to introduce crosslinking. A twin-screw extruder was used to mix PCO and DCP uniformly.

Figure 5 illustrates the configuration of a co-rotating twin-screw extruder, highlighting the self-wiping, intermeshing screw elements and the material flow within the barrel.

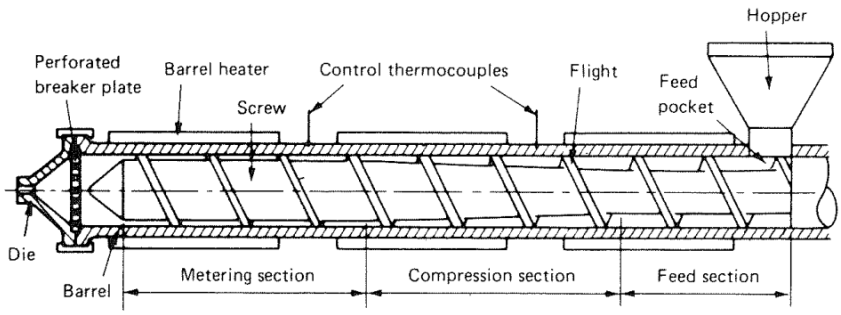

Figure 5: Schematic of the internals of a twin-extruder (15).

1.8 Previous work from MRG and material selection

This work builds on foundational research conducted by the Mather Research Group (MRG), which demonstrated that processing parameters—particularly cooling rate and annealing temperature—play a critical role in determining the crystallinity of semicrystalline polymers, and in turn, the efficiency of their shape memory effect (SME) (4). These findings established a direct relationship between thermal history and the mechanical behavior of shape memory polymers, emphasizing that crystallinity is not a fixed property but one that can be deliberately manipulated through processing. Motivated by this, the present study investigates how altering the crosslinking density affects crystallinity and SME performance in poly(cyclooctene) (PCO). Specifically, we tune the network structure by varying the amount of dicumyl peroxide (DCP), a thermal initiator that introduces covalent bonds between polymer chains. By systematically adjusting DCP concentration, we aim to understand how crosslinking influences fixity, recovery, and mechanical robustness—key performance factors for practical shape memory applications. This approach bridges prior insights with targeted material design strategies, contributing to the broader goal of engineering SMPs with customizable and reliable functionality.

1.9 Focus of This Thesis

For this thesis, samples are synthesized at varying DCP concentrations using different mixing techniques, including extrusion as shown above and a recently developed method that includes manually cutting and mixing the materials using a hot press. The samples are characterized using Differential Scanning Calorimetry (DSC) to measure Tg, Tm, and crystallinity, and Dynamic Mechanical Analysis (DMA) for mechanical properties by measuring storage modulus, loss modulus and tan(delta). Finally, we design a new protocol where we change prevailing conditions such as applied stress and crystallizing temperature during crystallization of the polymer and we evaluate the interplay between cross-linking, applied stress, and temperature in determining the system's mechanical properties.

PCO is a semicrystalline elastomer which shows shape memory behavior corresponding to a switching temperature (melting temperature) that is close to ambient room temperature. This makes crosslinked PCO useful for many practical applications. One potential application of these materials is in biomedical casts—specifically, in the development of shape-adaptive devices for clubfoot treatment, where tunable stiffness, fixity, and recovery are essential.

References

1. Pei, B., Wang, W., Feng, L., & Chen, Y. (13). Cross-linked polymers and their properties. *Polymer Bulletin*, 71(7), 1617–1626.

2. Rudin, A. (14). *The Elements of Polymer Science and Engineering*. Academic Press.

3. Victrex. (15). *Polymer crystallinity: A detailed overview*. https://www.victrex.com/en/blog/2017/polymer-crystallinity-hpp-explained-part-3.

4. Mather, P. T., Luo, X., & Rousseau, I. A. (16). Shape memory polymer research. *Annual Review of Materials Research*, 39, 445–471.

5. Kuraray Specialty Chemicals. (17). *What are elastomers?* https://www.elastomer.kuraray.com/us/blog/what-are-elastomers/.

6. S Chattopadhyay, *Proposal for Shape Memory Polymer Research Using Poly(cyclooctene)*, 2025.

7. Behl, M., & Lendlein, A. (18). Shape-memory polymers and their composites: Stimulus methods and applications. *Materials Science and Engineering: R: Reports*, 33(6), 106–147.

8. Lendlein, A., Jiang, H., Junger, O., & Langer, R. (19). Light-induced shape-memory polymers. *Nature*, 434(20), 879–882.

9. Xie, T. (18). Tunable polymer multi-shape memory effect. *Nature*, 464(21), 267–270.

10. Lendlein, A., & Kelch, S. (22). Shape-memory polymers. *Angewandte Chemie International Edition*, 41(10), 2034–2057.

11. Ratna, D., & Karger-Kocsis, J. (23). Recent advances in shape memory polymers and composites: A review. *Journal of Materials Science*, 43(1), 254–269.

12. Zhao, Q., Qi, H. J., & Xie, T. (24). Recent progress in shape memory polymer: New behavior, enabling materials, and mechanistic understanding. *Progress in Polymer Science*, 49–50, 79–120.

13. Gall, K., Dunn, M. L., Liu, Y., Finch, D., Lake, M., & Munshi, N. A. (19). Thermomechanics of the shape memory effect in polymers for biomedical applications. *Journal of Biomedical Materials Research Part A*, 73(3), 339–348.

14. Liu, Y., Gall, K., Dunn, M. L., McCluskey, P., & Finch, D. (25). Thermomechanics of shape memory polymer nanocomposites. *Mechanics of Materials*, 39(3), 211–226.

15. Meng, H., & Li, G. (26). A review of stimuli-responsive shape memory polymer composites. *Polymer*, 54(27), 2199–2221.

16. Pisani, S., Genta, I., Modena, T., Dorati, R., Benazzo, M., & Conti, B. (17). Shape-Memory Polymers Hallmarks and Their Biomedical Applications in the Form of Nanofibers. International Journal of Molecular Sciences, 23(3), 1290. https://doi.org/10.3390/ijms23031290.

17. C. Liu, *Preparation and Investigation of Tailored Shape Memory Polymers*, Ph.D. Dissertation, University of Connecticut, 2004.

18. L. H. Sperling, *Introduction to Physical Polymer Science*, 4th ed., Wiley-Interscience, 2005.

Chapter 2

Materials and Methods

2.1 Materials

2.1.1 Polycyclooctene (PCO)

Polycyclooctene (PCO) is a semicrystalline polymer that can show excellent shape memory properties. Its ability to undergo reversible crystallization and melting makes it a strong candidate for two-way shape memory applications. The long polymer chains contribute to their high crystallinity and mechanical strength, making it suitable for demanding industrial uses. PCO has a melting temperature that is close to room temperature making it suitable for biomedical applications amongst other things. PCO was selected due to its compatibility with crosslinking agents and its thermal behavior, which aligns well with the shape memory effect requirements.

2.1.2 Dicumyl Peroxide (DCP)

Dicumyl peroxide (DCP) is an organic peroxide commonly used as a crosslinking agent in polymer chemistry. Upon heating, DCP decomposes to form free radicals that initiate the formation of covalent bonds between PCO chains, thus stabilizing the network. For this study, DCP concentrations ranged from 1% to 5% by weight, allowing control over the degree of crosslinking. This control is crucial in balancing rigidity and flexibility in the final films.

2.2 Processing

2.2.1 Extrusion Blending

The polymer blends were processed using a twin-screw mini extruder to ensure thorough mixing and dispersion of the DCP and other additives. The extruder operated at a temperature of 80 °C and a screw speed of 80 rpm. To enhance homogeneity, the bypass valve was kept open

for 10 minutes before the extrudate was collected into a uniform ball shape. This method ensures consistent crosslinking behavior and improved mechanical and thermal performance in the final product. The samples were then cured in a hot press at 140 ºC for two hours to crosslink. This method was originally used, but compression molding gave cleaner samples with more control over the degree of crosslinking. Compression molding was used for the data in this thesis.

2.2.2 Compression Molding

DCP and PCO were first measured, and the PCO was shaped into a uniform ball by heating it in an oven at 80 °C. This ball was then placed in a hot press and flattened into a film at 90 °C. The film was folded in half, with the DCP evenly sprinkled between the layers, and pressed again. This process—pressing, cutting into quarters, folding, and reheating—was repeated five times to ensure thorough mixing of the crosslinking agent throughout the polymer matrix. Once the mixture was homogenous, it was placed between Kapton spacers and subjected to a final hot-pressing step at 140 °C for 2 hours to complete the crosslinking and form the final film.

2.2.3 Gel Fraction Analysis

Gel fraction analysis was used to quantify the degree of crosslinking in the films. The crosslinked films were immersed in a suitable solvent for an extended period to dissolve the uncrosslinked portion. The remaining insoluble gel was dried and weighed, and the gel fraction was calculated as the ratio of the insoluble portion to the initial mass. A higher gel fraction indicates a more densely crosslinked network. The purpose of this procedure is to determine the insoluble fraction, which the calculations, pictures from the procedure, and results are shown later in this thesis. This was how we quantified the samples as “high”, “medium”, or “low” concentration.

2.2.4 Differential Scanning Calorimetry (DSC)

Differential Scanning Calorimetry (DSC) was conducted using a TA Instruments DSC Q2000 to evaluate the thermal transitions and crystallization behavior of the samples. Each film sample (2–3 mg) underwent a heating cycle up to 100 °C to remove prior thermal history, followed by cooling to -50 °C and reheating to 100 °C at 10 °C/min. The heat flow curves revealed melting and crystallization peaks, which were integrated to determine enthalpy changes. With increased DCP content, crystallinity decreased, indicating that crosslinking reduced the mobility of polymer chains and hindered crystalline region formation.

2.3 Dynamic Mechanical Analysis (DMA)

2.3.1 Characterization DMA

Standard DMA tests were performed to assess the mechanical response of the films under oscillatory stress across a range of temperatures. A procedure of heat, cool, heat was applied to a strip sample. Parameters such as storage modulus (E'), loss modulus (E''), and tan delta (δ) were recorded to evaluate the stiffness and damping behavior of the crosslinked films.

2.3.2 Shape Memory DMA

To assess the shape memory characteristics, DMA was performed through a controlled thermomechanical cycle. Samples were deformed above the transition temperature, cooled under strain to fix the temporary shape, and then reheated to observe shape recovery. The effectiveness of shape recovery was quantified and compared across different DCP concentrations.

2.3.3 Isothermal Crystallization

Isothermal crystallization experiments were performed using DMA to understand the time-dependent crystallization behavior of the films at fixed temperatures. This method helped to

investigate the nucleation and growth rates of crystalline regions and how crosslinking density affects these kinetics.

Chapter 3

Results

Figure 6: Post-cured film of polycyclooctene (PCO) crosslinked with 4 wt% dicumyl peroxide (DCP), demonstrating uniform morphology following thermal treatment.

To begin with, we mixed PCO pellets with the DCP in required quantities, extrusion blended and then cured them at 140 ºC for two hours in a hot press. Curing ensures crosslinking of the chains and network formation. In Figure 6, we show a sample post curing. Visual inspection confirms that the film maintained structural integrity throughout the crosslinking process, with no apparent warping, cracking, or phase separation. This consistency indicates successful peroxide-initiated crosslinking and sets the stage for downstream thermal and mechanical analysis.

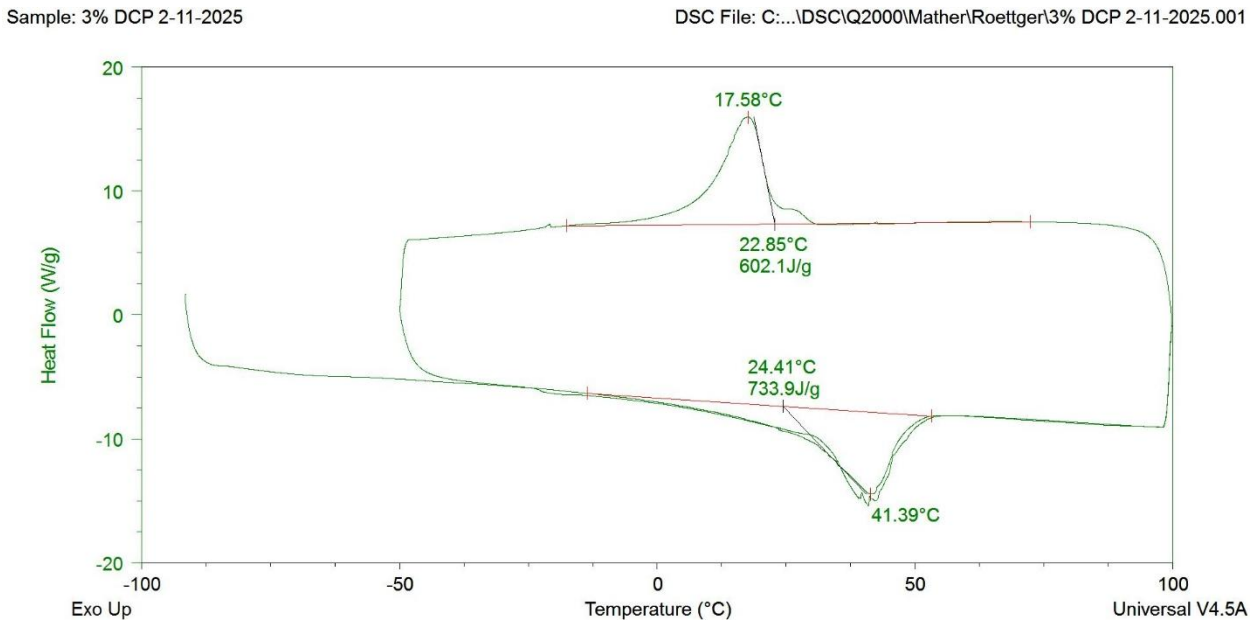

Figure 7: Differential scanning calorimetry (DSC) thermogram of the 3% DCP crosslinked PCO sample before solvent extraction. The curve shows the melting and crystallization transitions used to evaluate thermal behavior and crystallinity prior to removal of soluble polymer fractions.

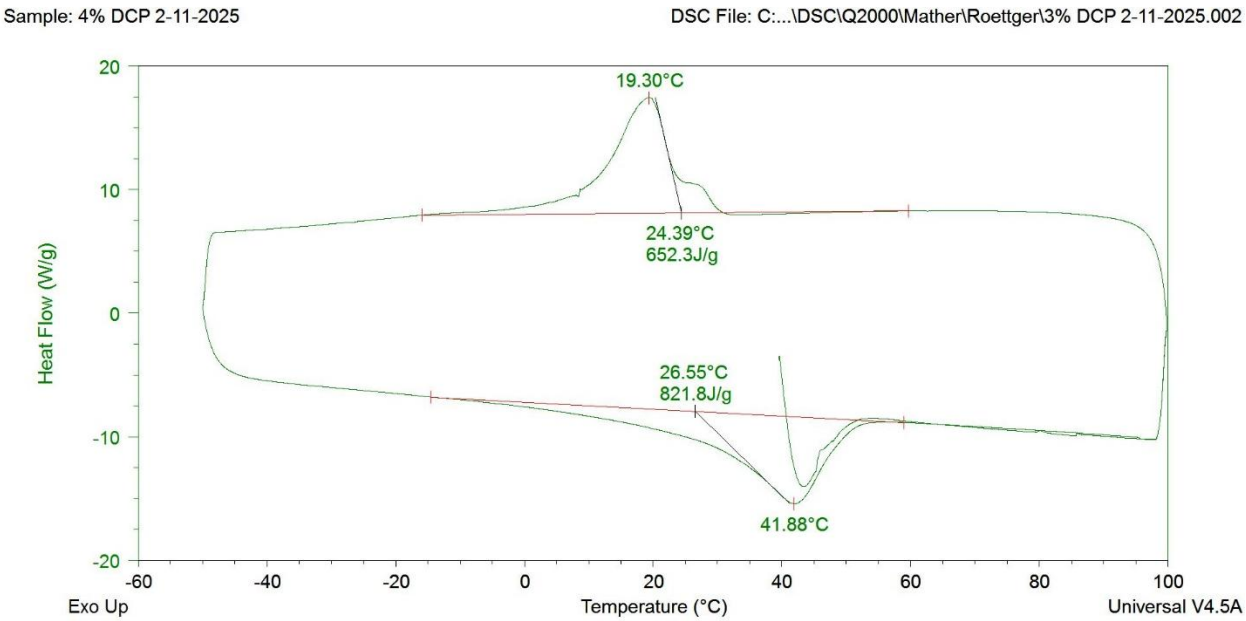

Figure 8: Differential scanning calorimetry (DSC) thermogram of the 4% DCP crosslinked PCO sample before solvent extraction. The curve shows the melting and crystallization transitions used to evaluate thermal behavior and crystallinity prior to removal of soluble polymer fractions.

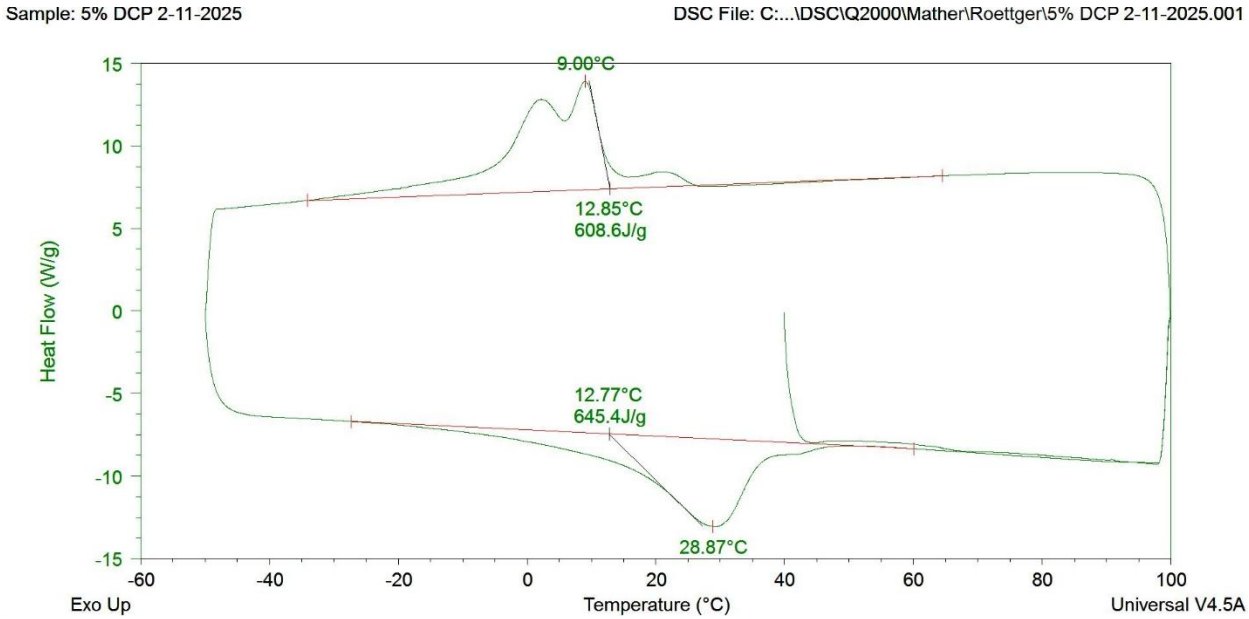

Figure 9: Differential scanning calorimetry (DSC) thermogram of the 5% DCP crosslinked PCO sample before solvent extraction. The curve shows the melting and crystallization transitions used to evaluate thermal behavior and crystallinity prior to removal of soluble polymer fractions.

Next, to characterize the samples, we perform DSC on the various crosslink density samples as shown in Figure 7, 8, and 9 for 3%, 4%, and 5% DCP concentration respectfully. Each figure shows a full thermal cycle including the cooling and the second heating cycle for characterization of melting and crystallization temperatures. The melting temperature (Tm) on average decreases with increasing crosslink density as can be seen from the figures: 3% melts around 41 °C, 4% near 42 °C, and 5% drops to approximately 29 °C. We do observe double peaks in the isotherm which we inspect further.

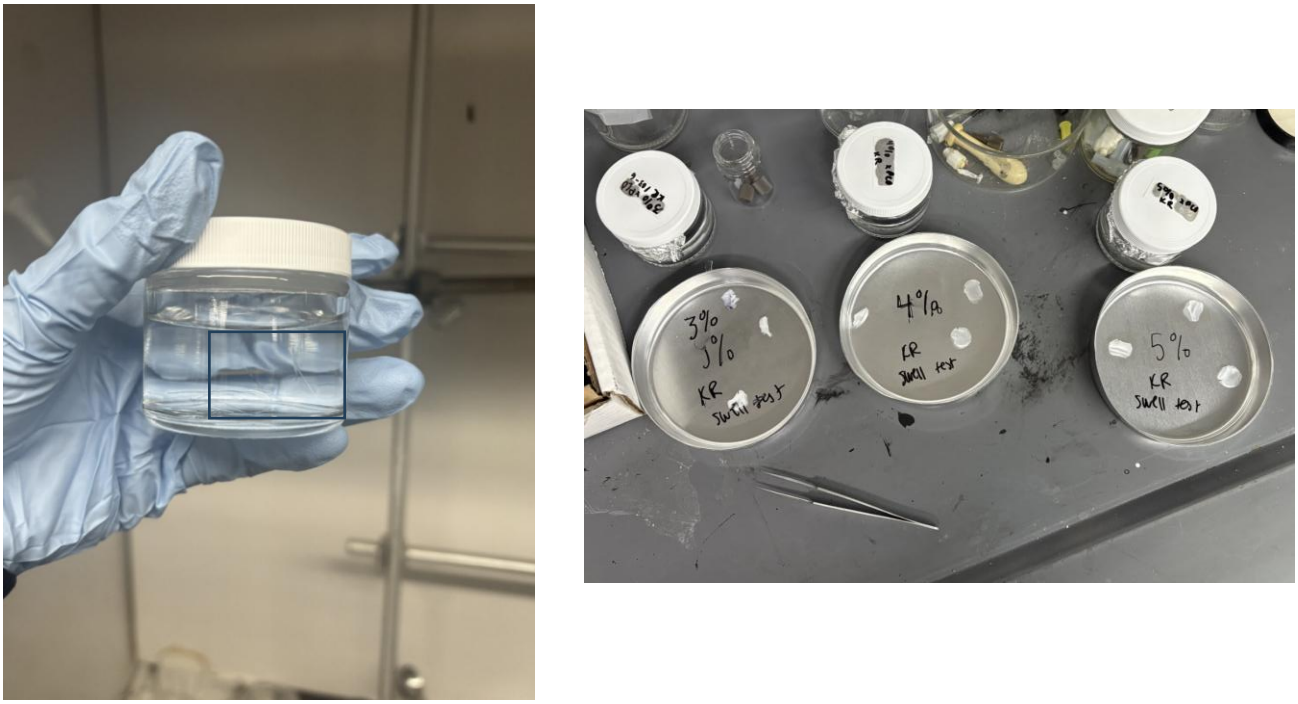

Figure 10: Gel fractioning setup for PCO samples crosslinked with 3%, 4%, and 5% DCP, showing both the swelling step and the dried gel fractions after extraction.

A standard method to quantify the degree of crosslinking in polymer networks is to measure the gel fraction via solvent extraction. In this study, samples were submerged in tetrahydrofuran (THF) for one week, with the solvent refreshed once midway to ensure complete extraction. During this process, uncrosslinked (soluble) polymer chains dissolve into the solvent, while the crosslinked (insoluble) network remains intact. Panel (a) shows a side view of a 4% DCP sample during the swelling step. As the sample begins to dissolve, it becomes transparent, making it difficult to visualize, but the swollen network can be seen within the black box. Panel (b) shows the dried samples after the soak, arranged by DCP content. The material that remained

after drying corresponds to the gel fraction, reflecting the extent of crosslinking in each formulation.

Table 1: Measured gel fraction for 3%, 4%, and 5% DCP crosslinked PCO samples. Higher DCP content resulted in increased insoluble mass fraction, consistent with greater crosslinking.

DCP wt %	Sample #	Pre-Swell Test Mass (mg)	Post-Swell Test Mass (mg)	Ratio	x 100%
	1	12.8	10.3	0.805	80.5
	2	14.4	11.5	0.799	79.9
3	3	12.3	10.2	0.829	82.9
	1	12	11.3	0.942	94.2
	2	16.7	16	0.958	95.8
4	3	13.6	13	0.956	95.6
	1	17	15.8	0.929	92.9
	2	16.5	15.4	0.933	93.3
5	3	16.9	15.6	0.923	92.3

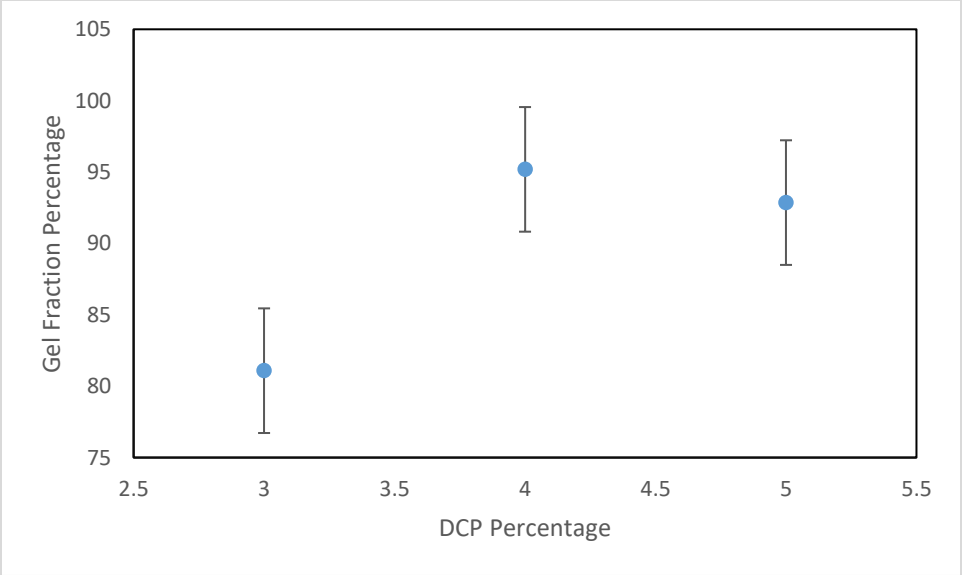

Figure 11: Gel fractioning results plotted.

We show the results of the gel fraction analysis in Figures 11 and 12. As expected, the gel fraction increases with the increasing weight percent of DCP added. Unexpectedly, though, the 4% DCP sample exhibited the highest gel content, indicating a well-crosslinked network. We do not have an explanation for the 4% sample having a higher gel fraction than the 5% sample.

Nevertheless, for the rest of the thesis, we will refer to the 4% DCP samples as “high” crosslink density sample, 5% as the medium and 3% as the low crosslink density samples.

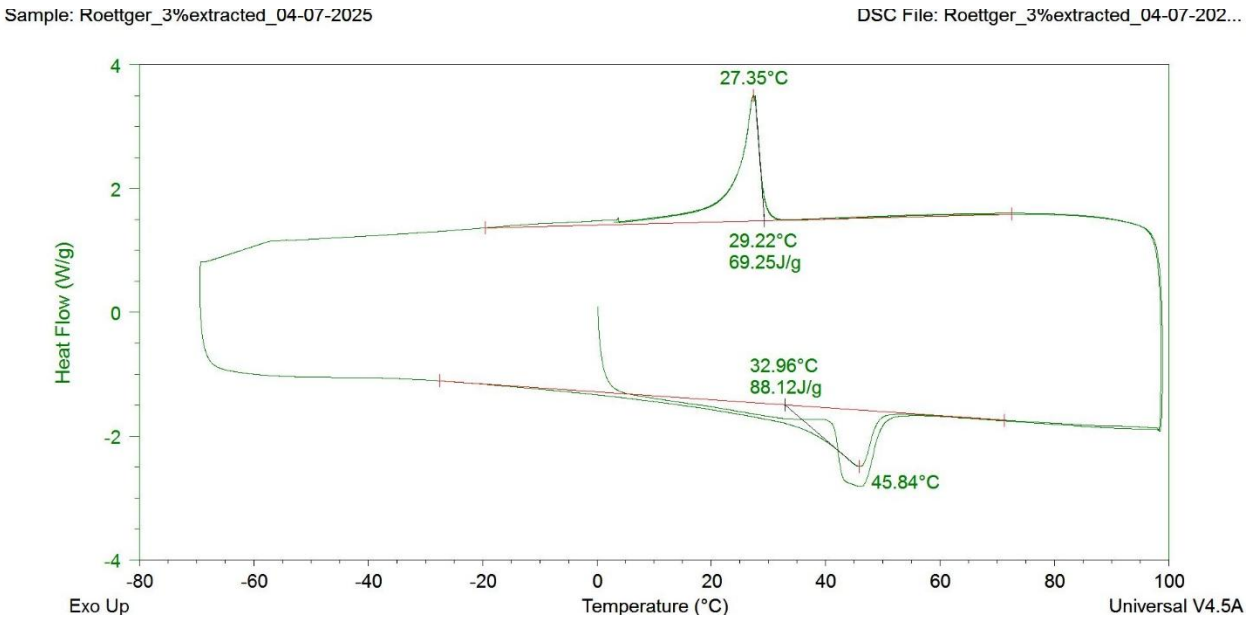

Figure 12: Differential Scanning Calorimetry (DSC) results of 3% DCP crosslinked PCO after extraction, showing a preserved melting transition around 45 °C. The second heating trace is annotated with a T_M of 45.84 °C.

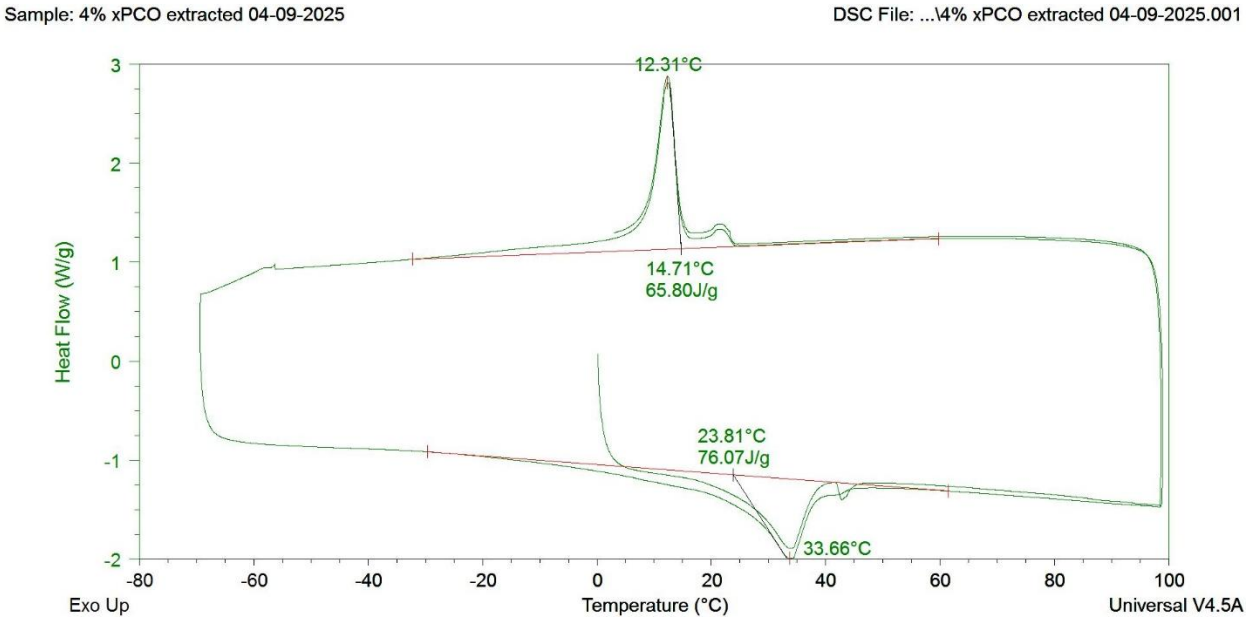

Figure 13: Differential Scanning Calorimetry (DSC) results of 4% DCP crosslinked PCO after extraction, showing a preserved melting transition around 34 °C. The second heating trace is annotated with a T_M of 33.36 °C.

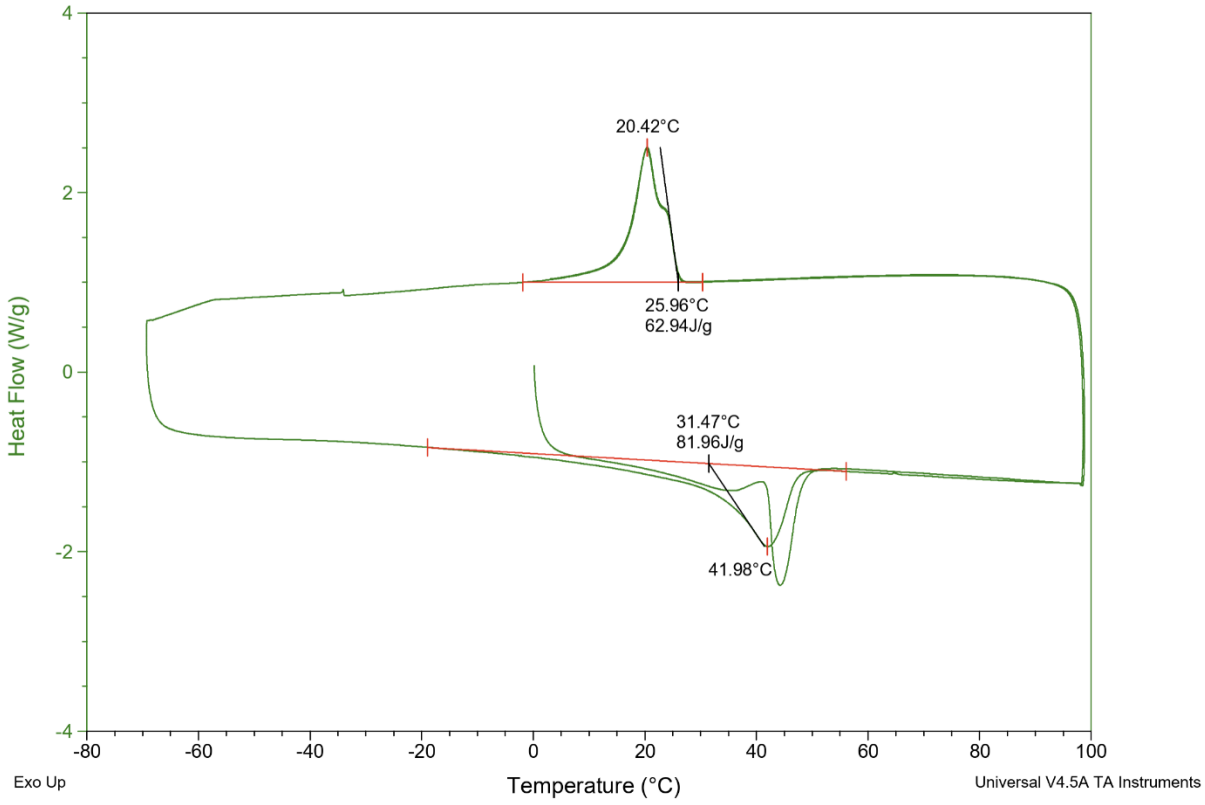

Figure 14: Differential Scanning Calorimetry (DSC) results of 5% DCP crosslinked PCO after extraction, showing a preserved melting transition around 32 °C. The second heating trace is annotated with a T_M of 31.47 °C.

We see that the crystallization and melting temperatures remain the same post extraction. However, some of the double peaks observed in the isotherm previously (in figure 7, 8, and 9) are not observed post extraction. We hypothesize that the loosely connected polymer strands in the non-extracted samples were the cause for the extra peaks in the isotherms.

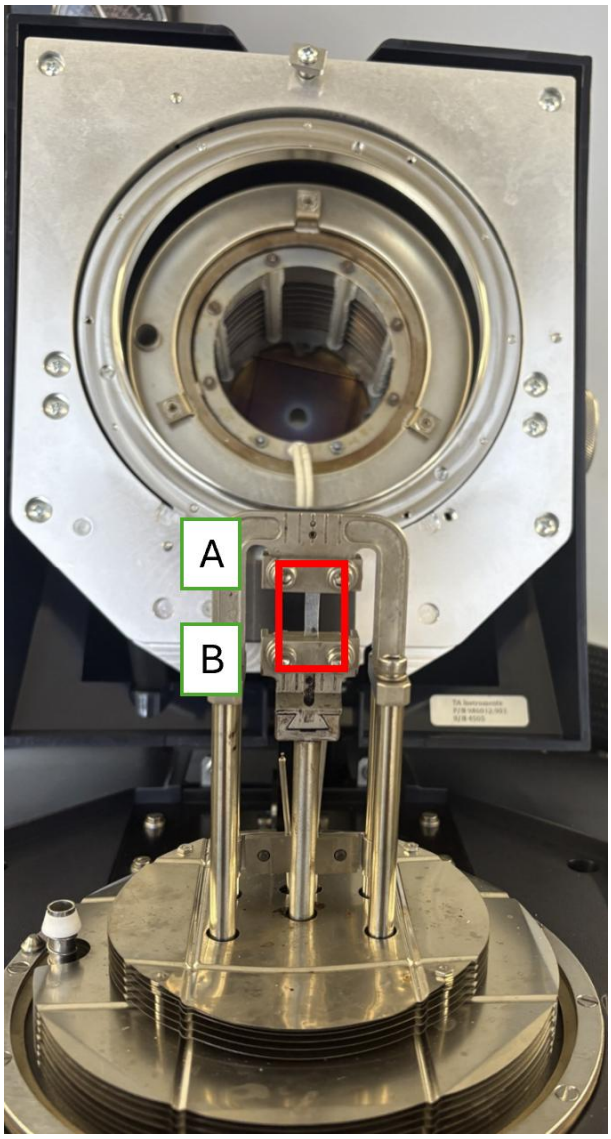

Figure 15: 4% extracted dog bone loaded into the DMA machine. The red box indicates the physical dogbone. A is the stationary grip and B is the oscillatory grip.

To characterize thermomechanical properties of the samples, we use Dynamic Mechanical Analysis (DMA). In figure 15, we show a dog-bone mounted into the DMA.

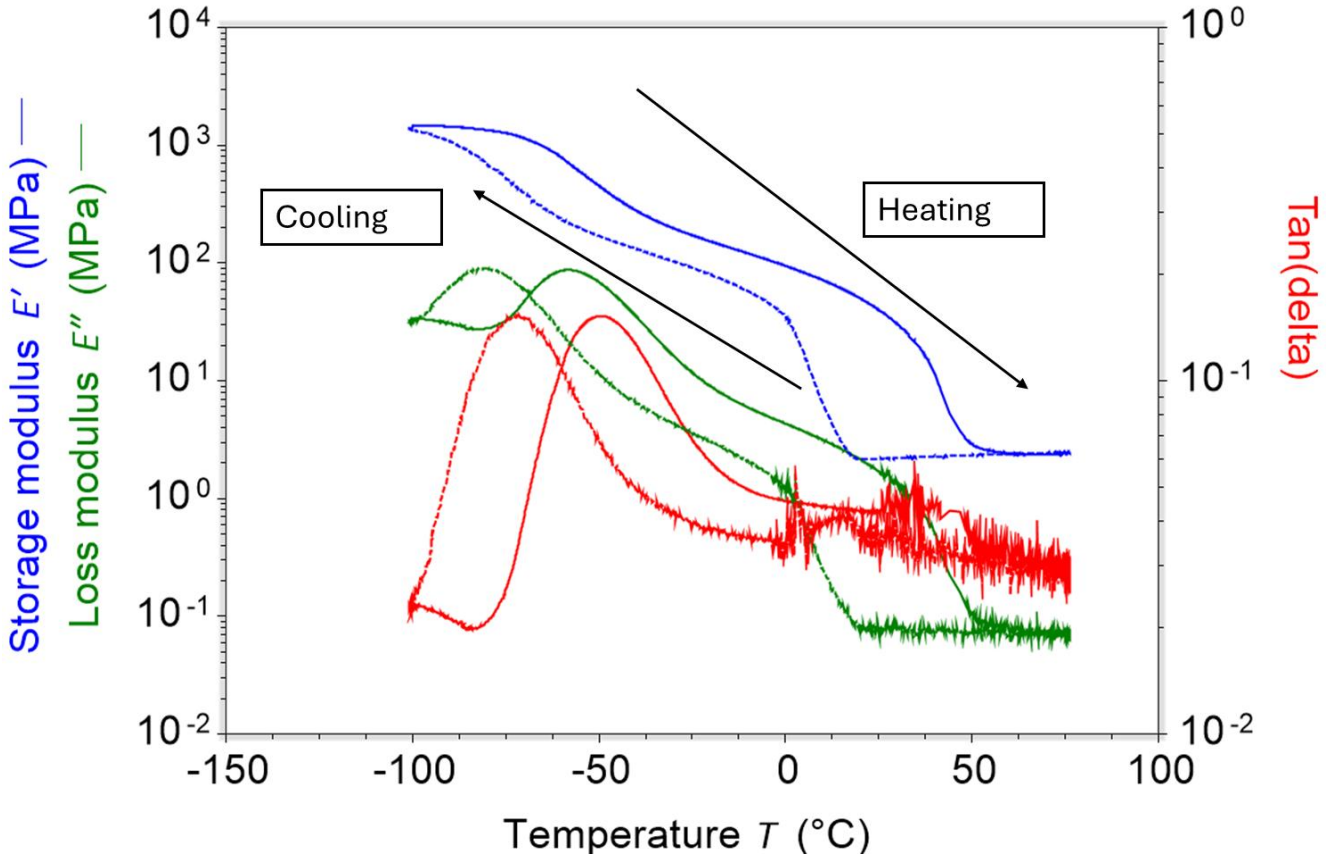

Figure 16: Thermal mechanical properties of medium crosslinked PCO characterized by DMA at a heating rate of 3 ºC/min. This is the entirety of the normal DMA run, not just the snippet of the heating curve.

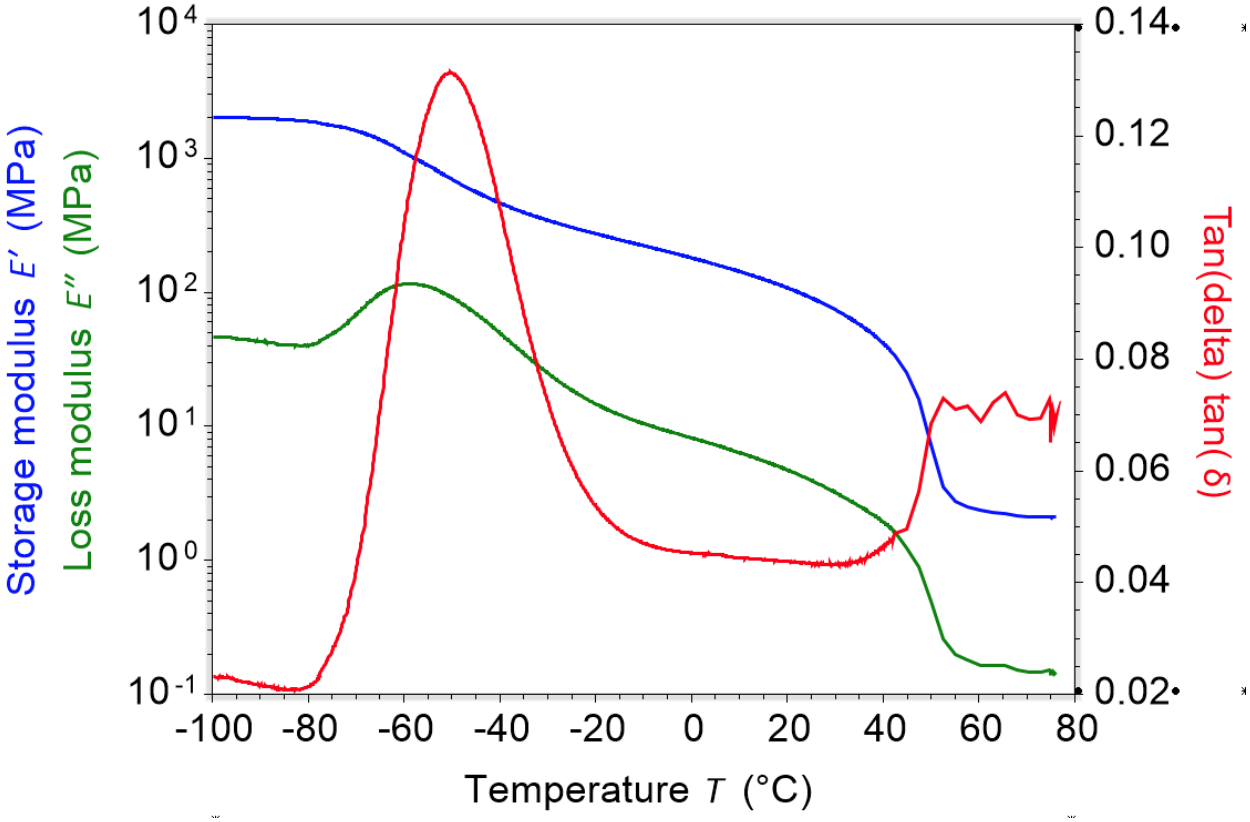

Figure 17: Thermal mechanical properties of 3% crosslinked PCO characterized by DMA at a heating rate of 3 ºC/min. This was the third run in a set of three for repetition. Blue line: storage modulus; green line: loss modulus; red line: tan delta.

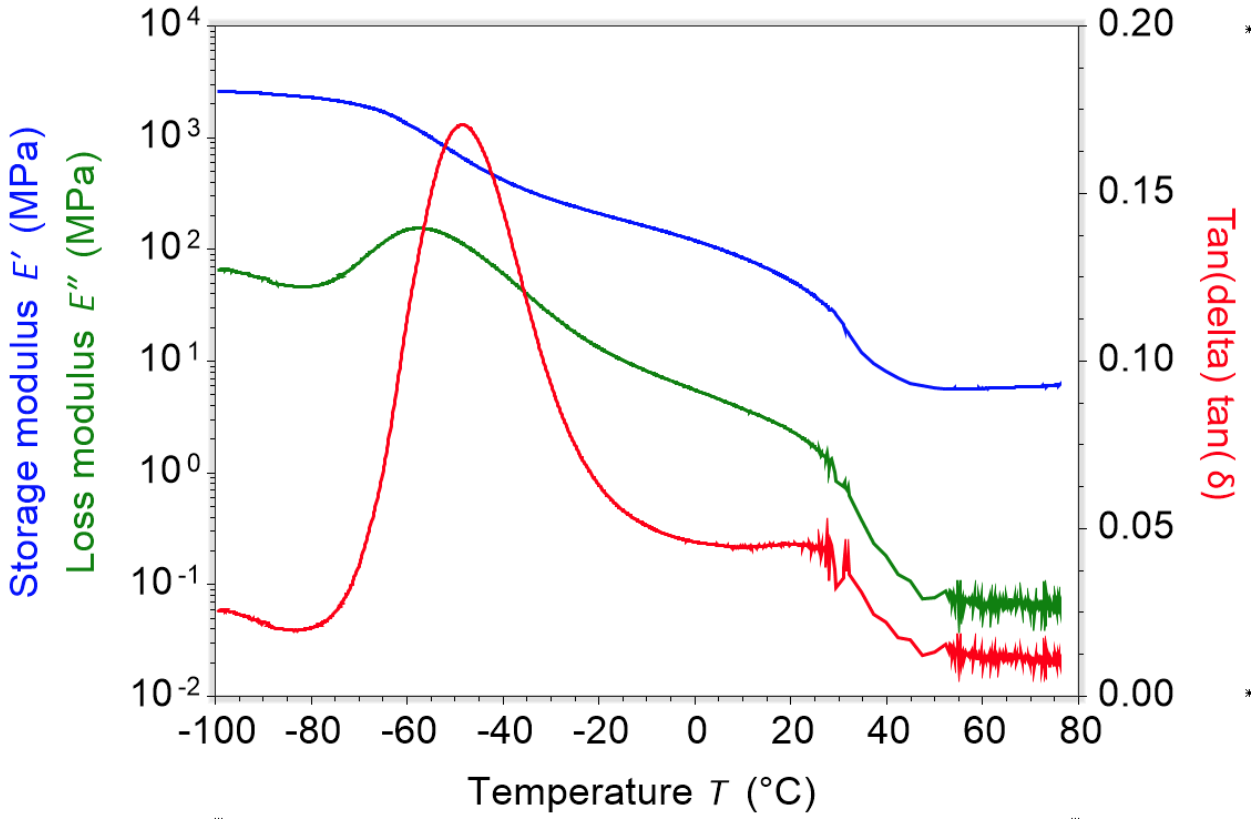

Figure 18: Thermal mechanical properties of 4% crosslinked PCO characterized by DMA at a heating rate of 3 ºC/min. This was the third run in a set of three for repetition. Blue line: storage modulus; green line: loss modulus; red line: tan delta.

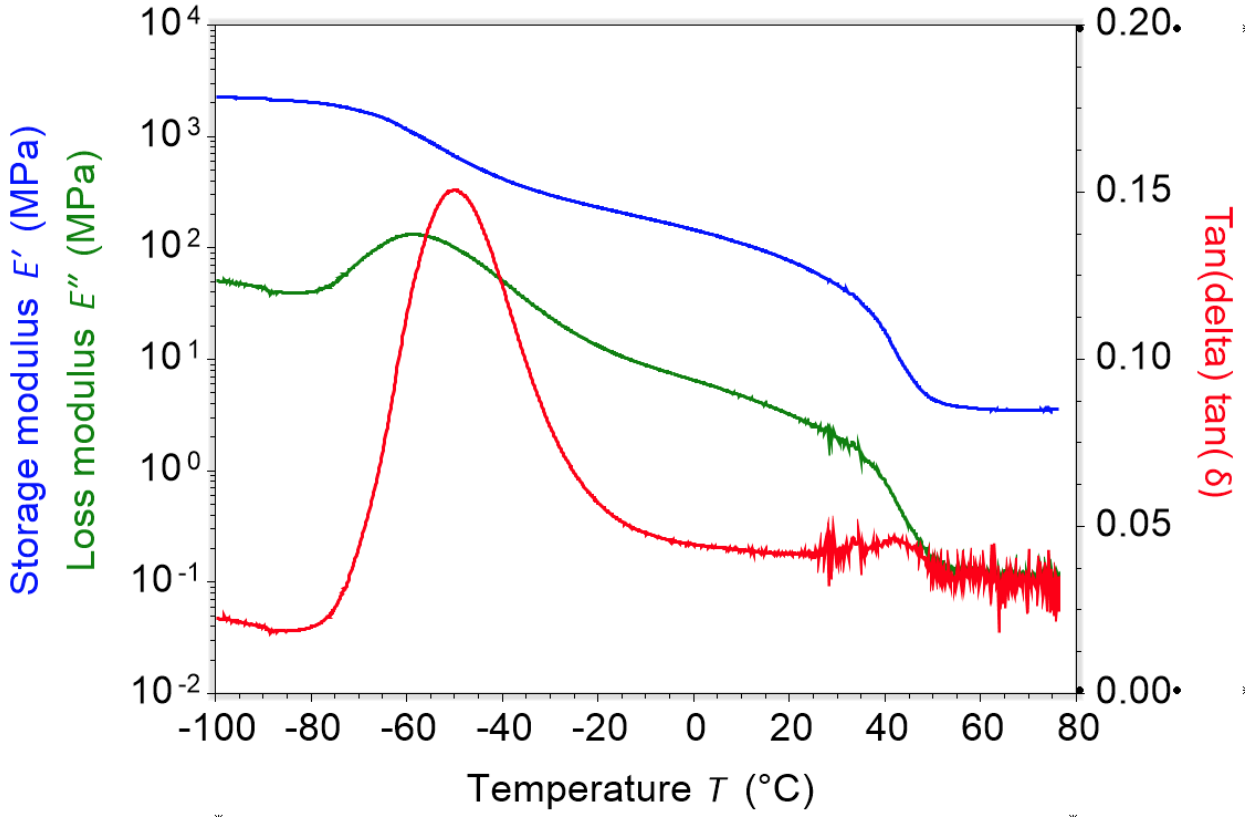

Figure 19: Thermal mechanical properties of 5% crosslinked PCO characterized by DMA at a heating rate of 3 ºC/min. This was the third run in a set of three for repetition. Blue line: storage modulus; green line: loss modulus; red line: tan delta.

To characterize the samples, we utilized the DMA, and the results are shown above. The procedure is as follows. First, we characterize the thermal behavior of the samples in the DMA by observing the storage and loss moduli of the samples over a temperature range of –100 ºC to 150 ºC. We first heat the sample to 75 ºC beyond the melting temperature of the sample followed by cooling to -100 °C. Finally, we heat the sample to 150 °C and we observe the storage modulus (E′), loss modulus (E″), and tan delta (tan δ) in this second heating cycle. The second heating cycle is presumed to be free of prior thermal history. E′ represents the elastic response of the material, E″ corresponds to the energy lost as dissipation during cyclic deformation, and tan δ is a ratio of E″ to E′ that reflects damping. The glass transition temperature (Tg) is most accurately identified from the peak in the loss modulus (E″), as this corresponds most closely with the Tg measured by DSC. The peak in tan δ can also be used as an indicator of Tg, while the sharp drop in the storage modulus (E′) at higher temperatures is typically used to approximate the melting temperature (Tm). We match the melting temperatures obtained from DMA to those obtained via DSC characterization.

Among the three crosslinking levels, Tg remains relatively unchanged, which is consistent with expectations since DCP crosslinking primarily influences crystalline domains rather than the amorphous phase. As DCP content increases, Tm decreases—from approximately 41 °C in the 3% sample to around 29 °C in the 5% sample—indicating suppression of crystallinity with higher crosslink density. The rubbery plateau modulus (E′ at high temperatures beyond melting) increases with crosslink density, demonstrating that higher crosslinking results in a stiffer network. These observations follow expected trends previously reported in the group and help confirm that crosslink density can be used to tune thermal and mechanical performance.

All DMA figures now include only one representative heating curve per crosslink level. These curves were selected based on closeness to the average of three repetitions to minimize redundancy and emphasize the comparative trends.

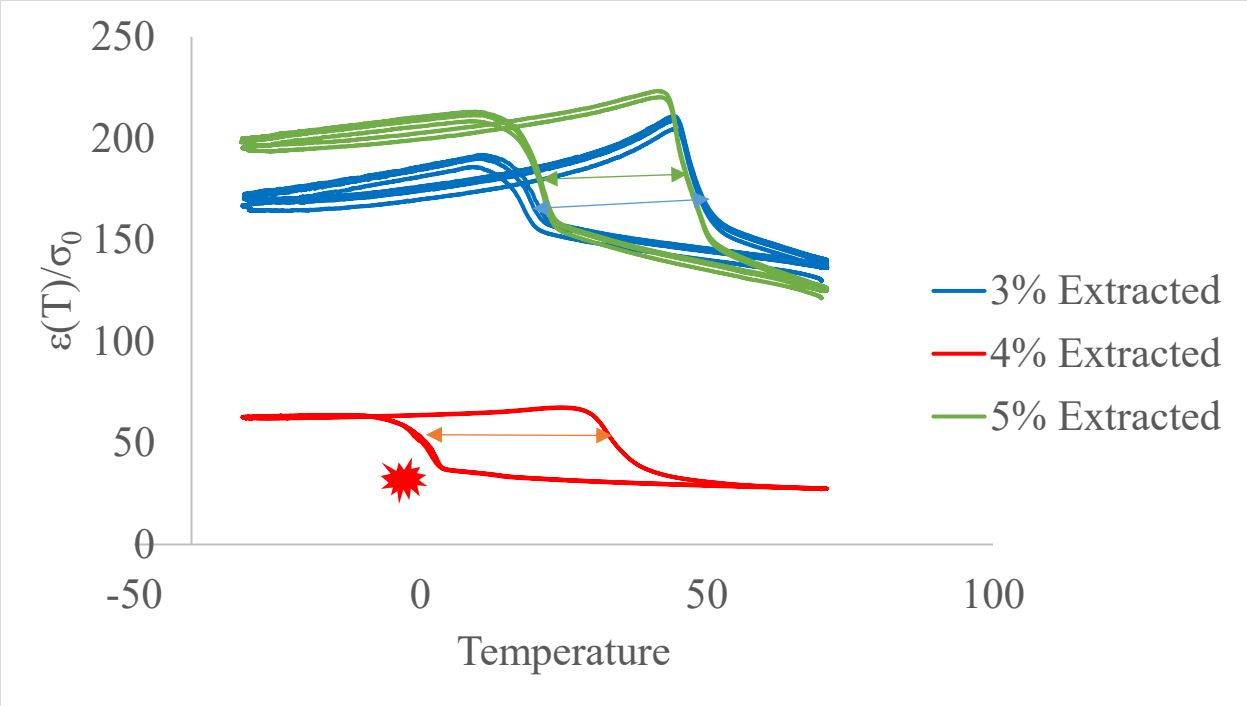

Figure 20: Normalized shape memory cycles for 3%, 4%, and 5% crosslinked PCO, showing strain divided by stress to compare elastic response. Hysteresis reveals that heating and cooling behavior differ, with 4% showing the greatest magnitude and 3% the least. Asterisks mark the onset of crystallization upon cooling, which occurs at lower temperatures and with slower kinetics in more highly crosslinked samples.

To directly compare the shape memory behavior across formulations, normalized plots (actuation strain divided by applied tensile stress) were generated. This representation removes the effect of differing applied stresses and emphasizes the intrinsic network recovery. The 5% sample shows the steepest recovery curve, followed by 4%, then 3%, aligning with trends

observed in gel fraction and DMA data, confirming that shape recovery strength scales with crosslink density.

The hysteresis in each cycle reveals a clear difference between heating and cooling responses, with the 4% sample exhibiting the largest hysteresis loop and the 3% the smallest. Quantitatively, the temperature difference between contraction on heating and elongation on cooling was approximately 35 °C for the 3% sample, 30 °C for the 4% sample, and 45 °C for the 5% sample. These values indicate that increased crosslinking broadens hysteresis, reflecting slower crystallization kinetics and reduced network mobility. Asterisks in the plot mark the onset of crystallization during cooling, with more crosslinked samples (such as 5%) crystallizing more slowly and at lower temperatures under stress.

Now that we have characterized the two-way shape memory behavior of this system, we look more closely at the underlying crystallization behavior. Previous work has shown that crystallization-induced elongation in this system depends systematically on the applied stress during cooling (1). To explore this further, we designed a new protocol in which samples crystallize isothermally under constant stress, and we monitor the strain development throughout the process.

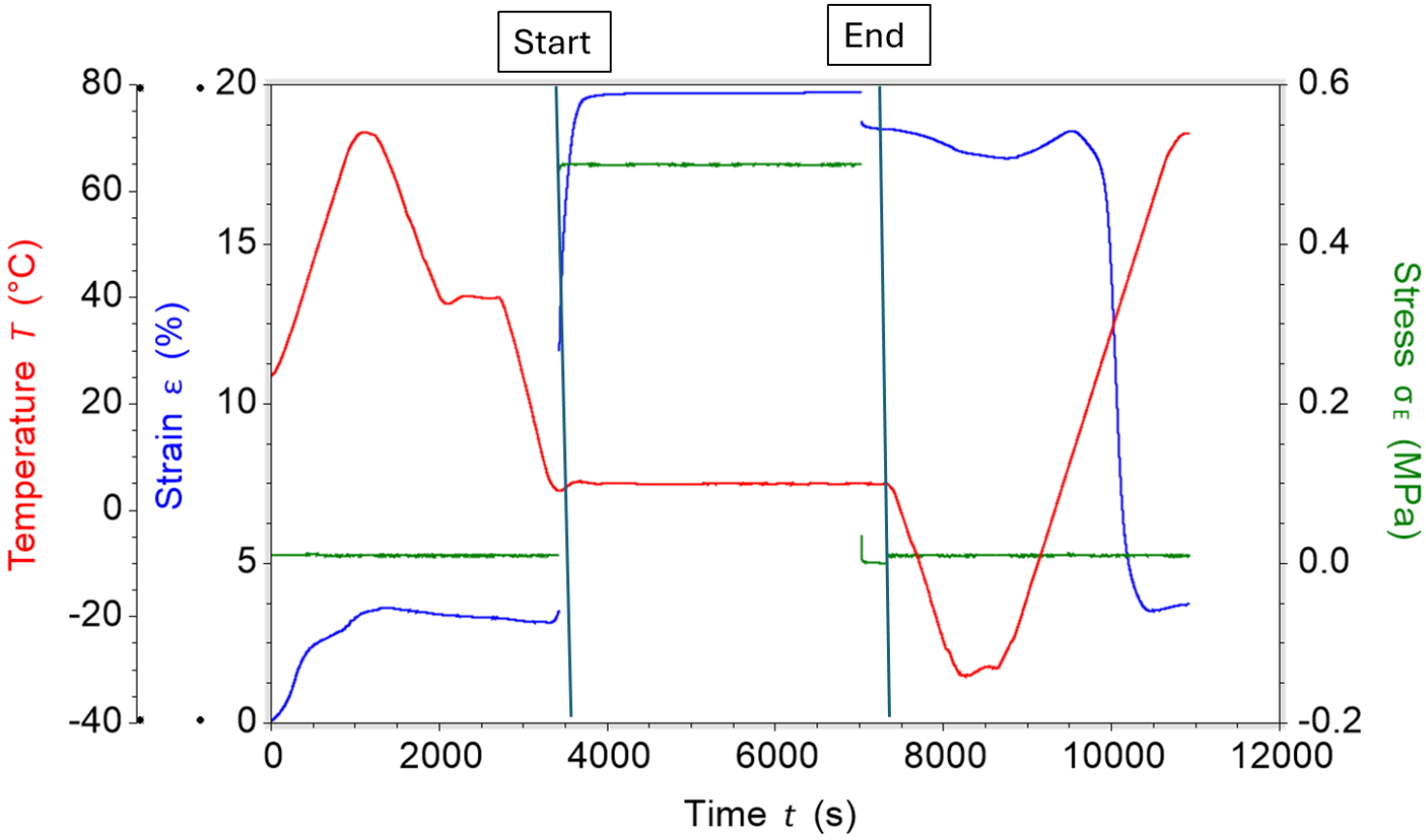

Figure 21: Shape memory DMA protocol showing strain (blue), temperature (red), and stress (green) over time. During the isothermal programming step, strain increases rapidly at first, then gradually slows and plateaus as the sample conforms to the applied stress. The shaded region marks the isothermal crystallization period, which is the focus of the following graphs.

In Figure 21, we show the shape memory protocol. During the isothermal hold, strain increases quickly at first and then gradually levels off as the sample finishes responding to the applied stress. From this point forward, all data shown is for the highest crosslink density sample ("high"). We picked a range of temperatures below the melting point and ran the isothermal crystallization protocol at each one to see how temperature affects the behavior.

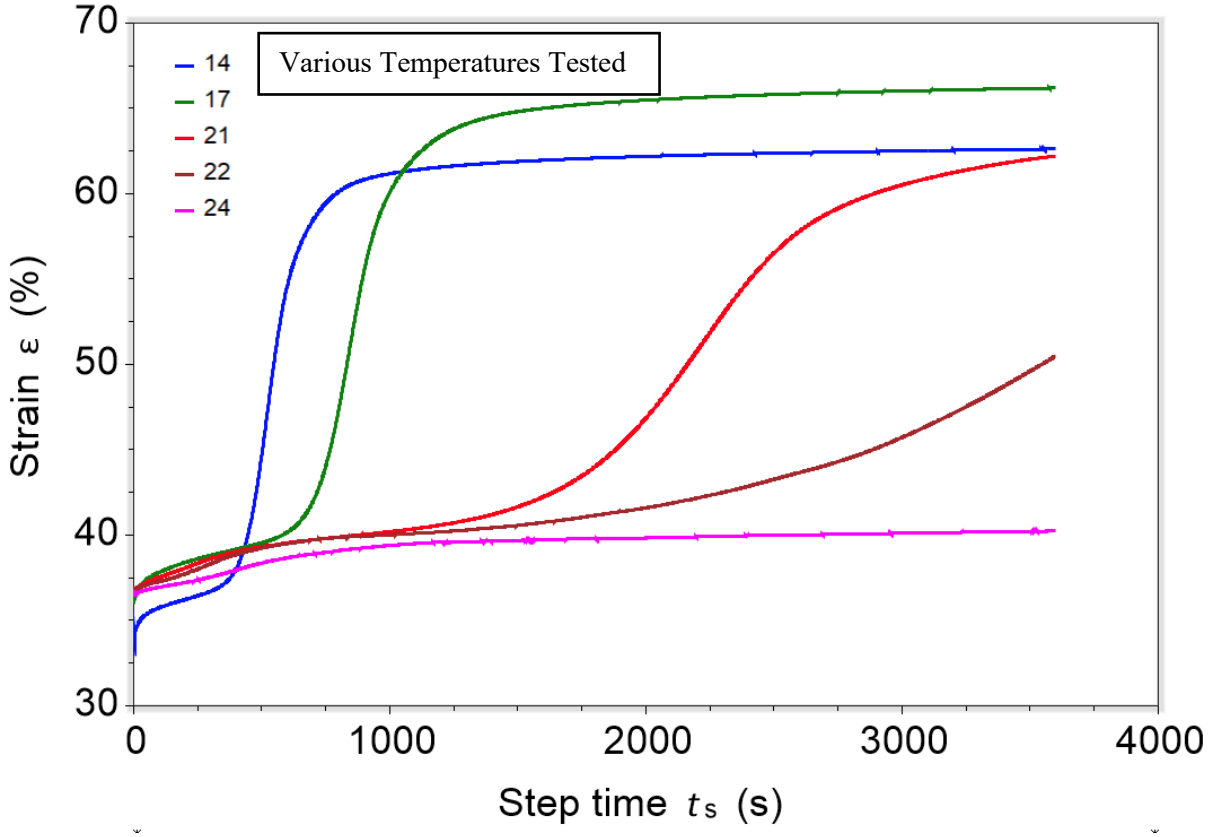

Figure 22: Strain evolution during isothermal crystallization of high crosslinked PCO under constant stress at various temperatures, highlighting the temperature dependence of stress-induced crystallization.

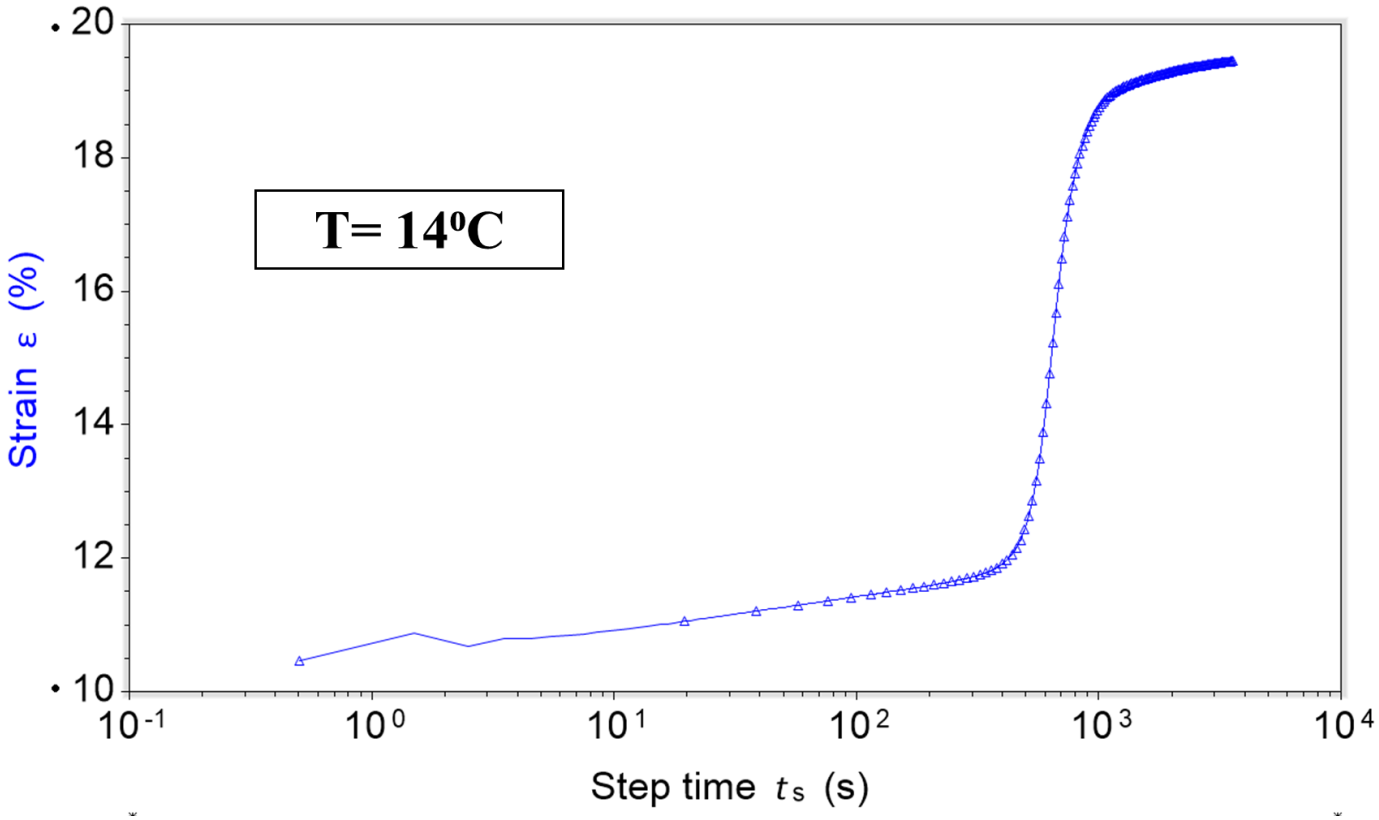

Figure 23: Strain evolution during a 1-hour isothermal hold at 14 °C for the high crosslink density sample.

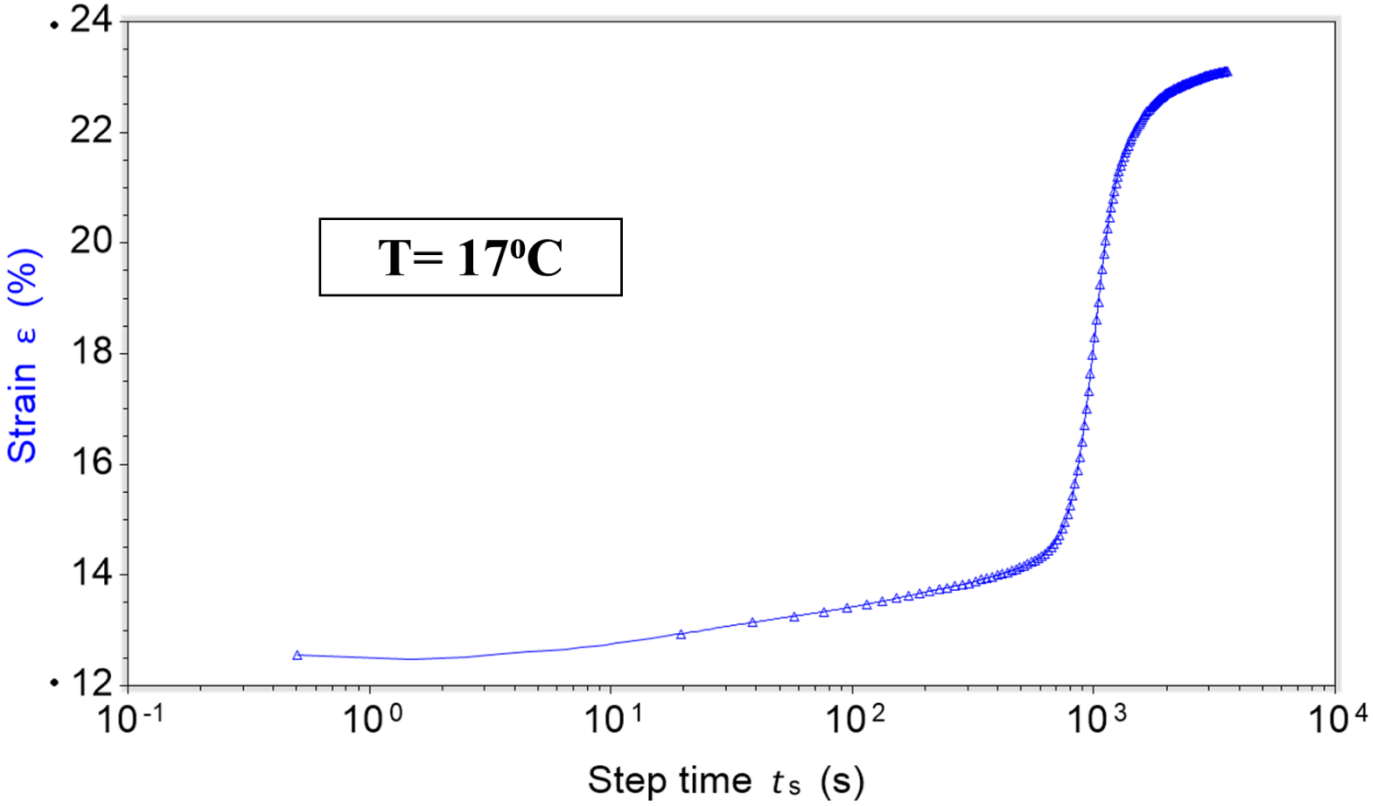

Figure 24: Strain evolution during a 1-hour isothermal hold at 17 °C for the high crosslink density sample.

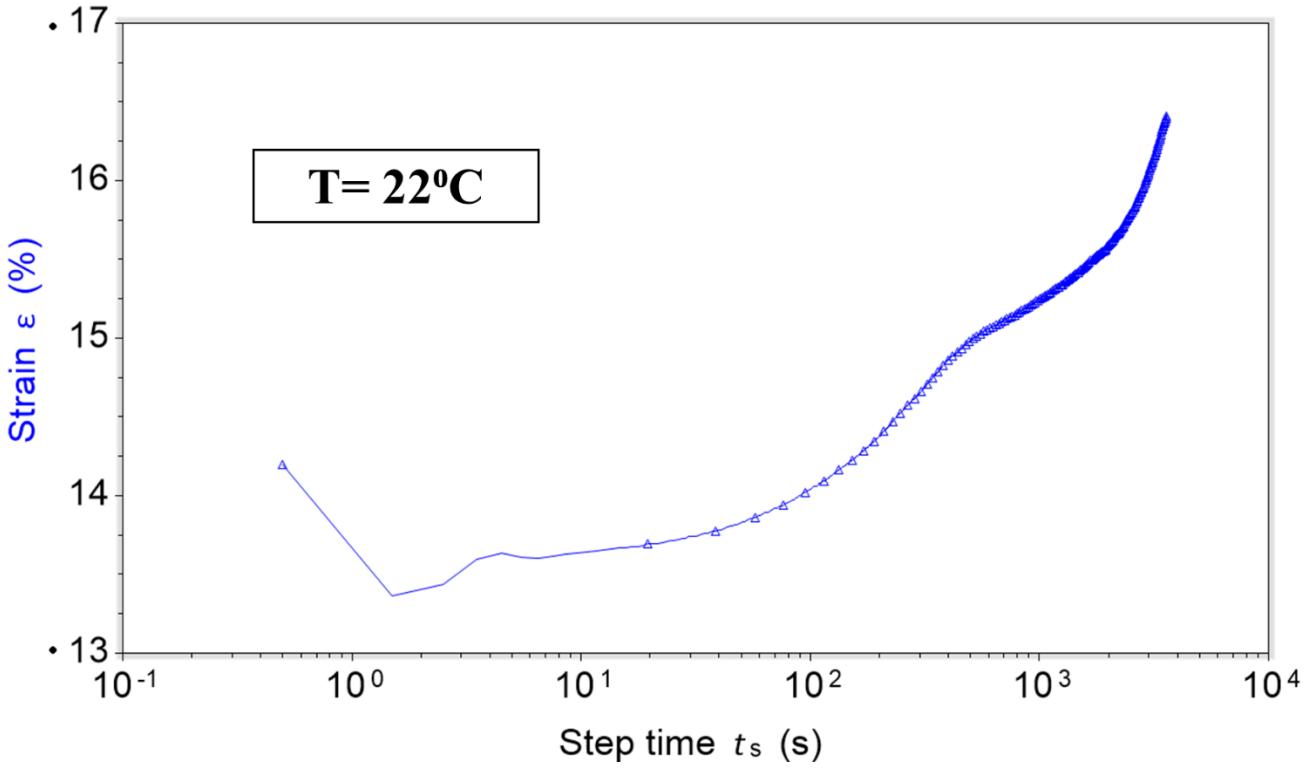

Figure 25: Strain evolution during a 1-hour isothermal hold at 22 °C for the high crosslink density sample.

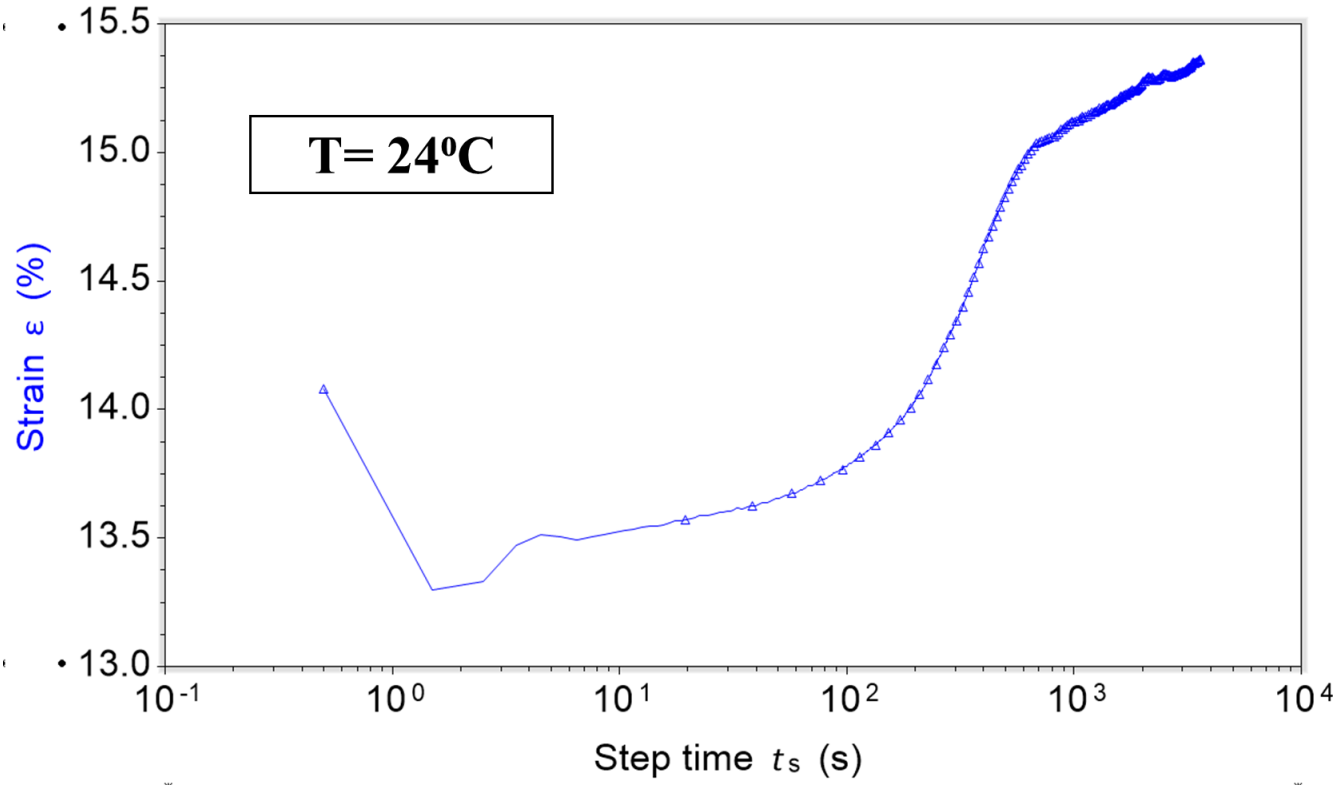

Figure 26: Strain evolution during a 1-hour isothermal hold at 24 °C for the high crosslink density sample.

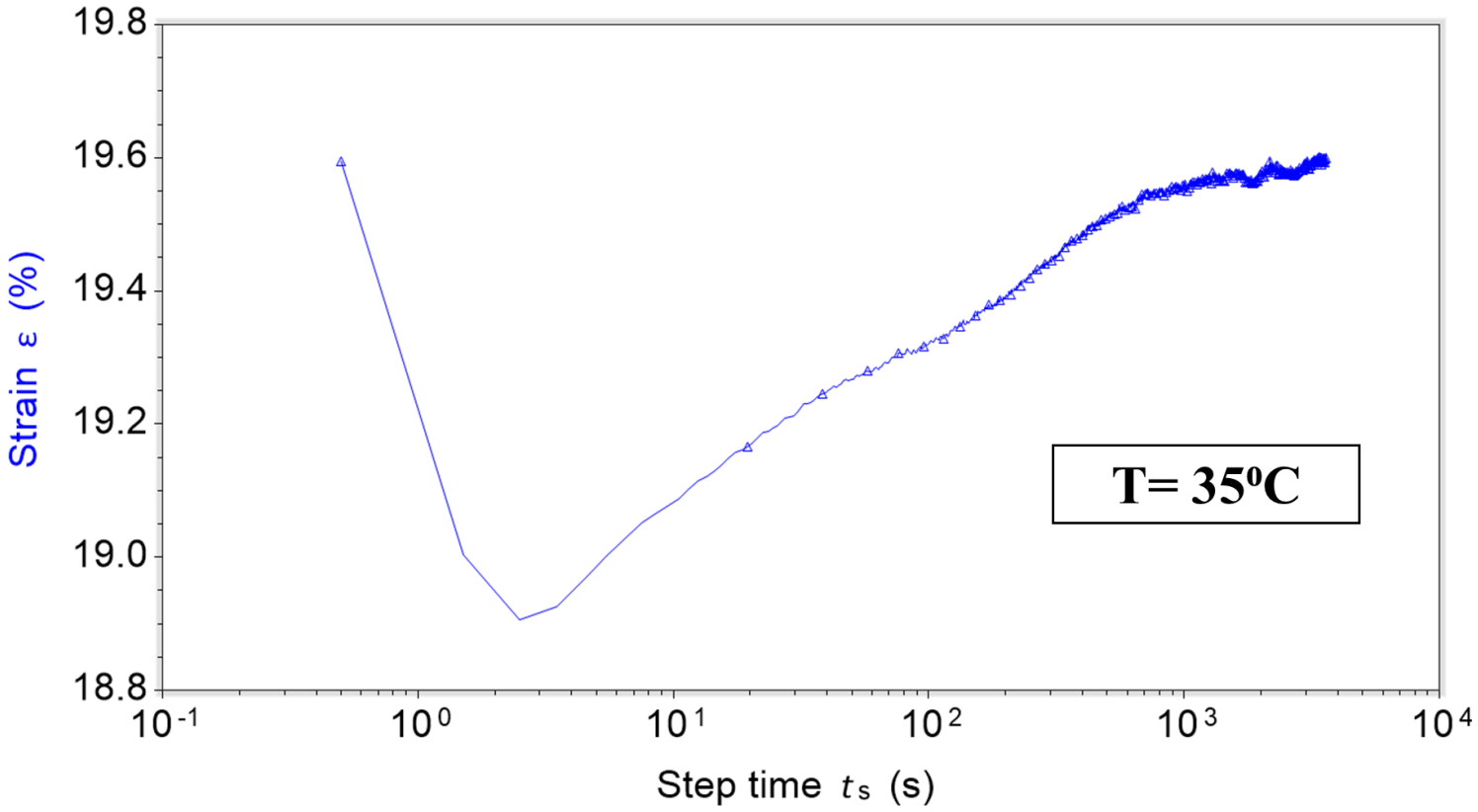

Figure 27: Strain evolution during a 1-hour isothermal hold at 35 °C for the high crosslink density sample.

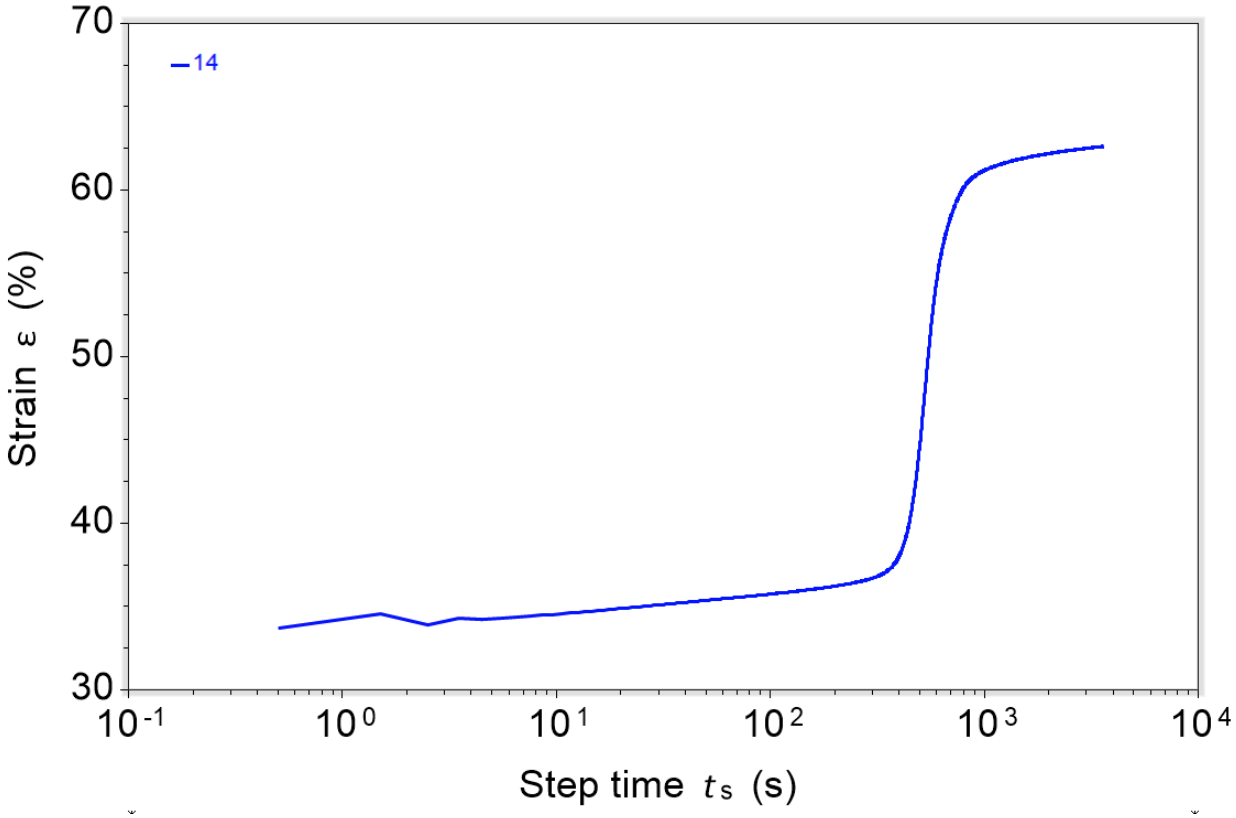

Figure 28: Semi-log plot of strain during isothermal crystallization at 14 °C, emphasizing the extended incubation period followed by a sharp increase in strain that reflects rapid crystallization onset and temperature-dependent kinetics.

In Figure 28, at 14 °C, the sample initially shows very little change in strain, which means that crystallization isn't happening right away. This period is called the incubation time, where the material is slowly organizing before crystals start to form. After this delay, the strain increases quickly, showing that crystallization happens rapidly once it begins. This behavior is clearer when the data is shown on a semi-log scale, which helps us see how long the material takes to start crystallizing and how fast it grows once it does.

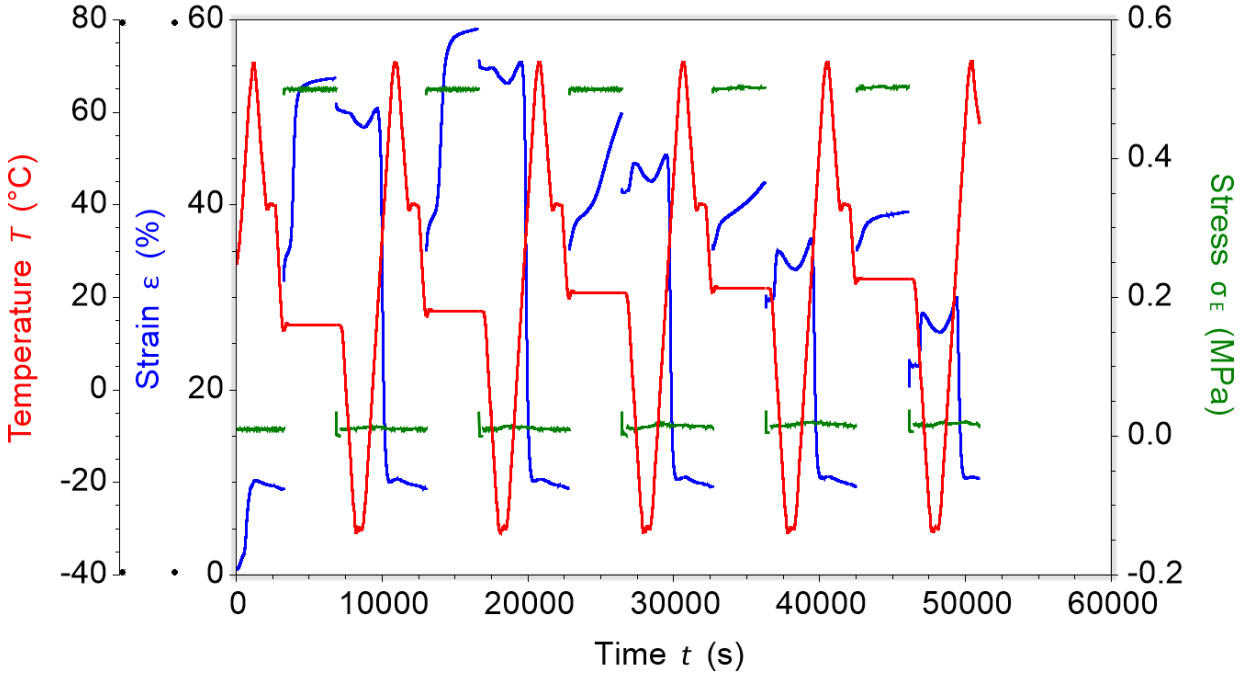

Figure 29: Isothermal crystallization experiments performed back-to-back at five different temperatures, showing the effect of temperature on strain response over time.

In Figure 27, we show isothermal crystallization at five different temperatures that run back-to-back. The difference in elongation behavior across these temperatures is striking and highlights how sensitive the system is to small temperature changes.

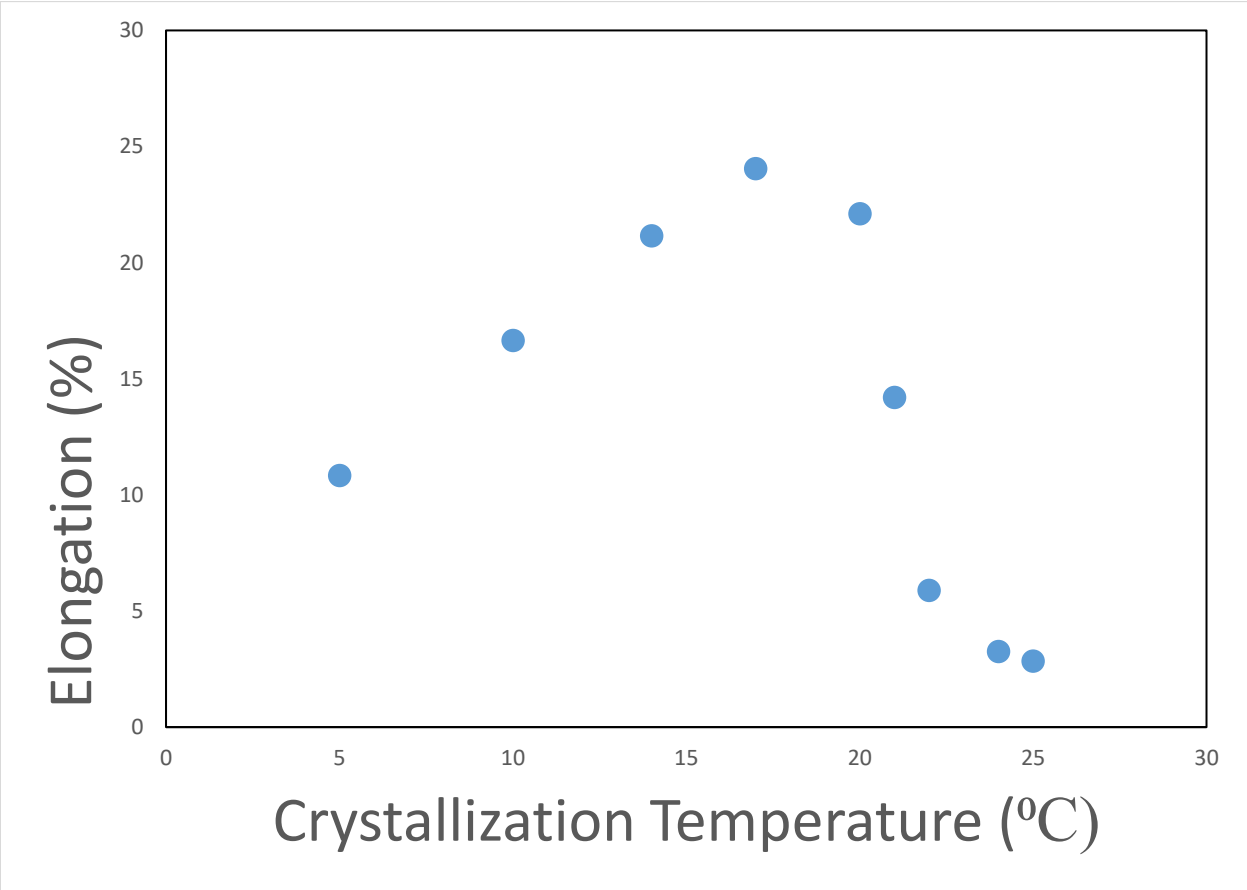

Figure 30: Elongation as a function of crystallization temperature ($T_{(iso)}$) for all conditions studied. Near the melting point, elongation shows strong sensitivity to temperature under a constant 0.5 MPa stress.

Finally, in Figure 30, we plot elongation as a function of crystallization temperature for all the temperatures studied in this thesis. Over a narrow temperature range near the melting point, the system shows a clear and sharp sensitivity to the applied temperature. All results were obtained under a constant stress of 0.5 MPa.

References

1. C. Liu, *Preparation and Investigation of Tailored Shape Memory Polymers*, Ph.D. Dissertation, University of Connecticut, 2004

Chapter 4

Applications and Future Directions

Based on the results presented in Chapter 3, crosslinked polycyclooctene (PCO) with tunable dicumyl peroxide (DCP) content shows promising thermomechanical and shape memory behavior. As the crosslink density increased, the materials became stiffer overall, and their ability to recover shape after deformation improved. This was clearly shown in the DMA results (Figures 16–19), where the storage modulus increased with DCP content, and in the shape memory test (Figure 20), where recovery became more complete and rapid with higher crosslink density. The tan delta peak remained in a similar temperature range across all concentrations, suggesting that the glass transition was not heavily affected by crosslinking. However, the melting region shifted lower with more crosslinking, indicating a suppression of crystalline domains.

These thermal trends were supported by DSC analysis, which showed melting peaks moving to lower temperatures and slight reductions in enthalpy with increased DCP. This further suggests that higher crosslink density limits crystallization, which plays a role in shape memory behavior. Together, the DMA and DSC results show that thermal and mechanical performance can be predictably tuned by changing the amount of DCP added.

One potential application for this material system is in biomedical casting devices, specifically for pediatric clubfoot treatment. Current casting methods require repeated manual adjustment or replacement of rigid casts to accommodate gradual changes in foot alignment. A shape memory-based cast made from crosslinked PCO could be pre-programmed into a deformed shape and then triggered (e.g., via heat) to gradually recover its original shape,

applying gentle corrective force to the foot over time. Because PCO has a melting transition near body temperature, the material could be activated in a safe and controlled way, especially in settings where direct thermal stimulation is possible. Additionally, the stiffness of the cast could be tuned by adjusting DCP concentration, allowing for different degrees of rigidity depending on treatment stage or patient size.

This thesis opens many interesting directions for future work. The isothermal crystallization under applied stress certainly requires more investigation to understand the interplay between stress, strain and temperature. It will also be interesting to explore whether and in what way does cross-link density variation affects this interplay. Additional experiments, along with repeated runs will be able to establish the observed trends robustly. Microstructure analysis using crystallographic techniques such as wide angle and small angle x-ray scattering will be useful in understanding how crystalline morphology is affected in correlation with the non-monotonic variation in the overall elongation that we observed in Figure 28. For application of this system as a biomedical cast, additional testing would include shape memory cycling over many thermal cycles, evaluation of recovery under constrained (realistic) deformation setups, and mechanical fatigue testing. Biocompatibility would also need to be assessed to move toward medical approval.

Overall, this thesis investigated the thermomechanical and shape memory properties of crosslinked PCO by controlling DCP concentration. The trends observed in DMA and DSC show consistent structure–property relationships, which provide a strong foundation that can be used for future applications in biomedical areas.